

University of California

Ernest O. Lawrence Radiation Laboratory

BRANCHING RATIOS IN K^+ MESON DECAY

TWO-WEEK LOAN COPY
This is a Library Circulating Copy
which may be borrowed for two weeks.
For a personal retention copy, call
Tech. Info. Division, Ext. 5545

Berkeley, California

16362
cy 2

DISCLAIMER

This document was prepared as an account of work sponsored by the United States Government. While this document is believed to contain correct information, neither the United States Government nor any agency thereof, nor the Regents of the University of California, nor any of their employees, makes any warranty, express or implied, or assumes any legal responsibility for the accuracy, completeness, or usefulness of any information, apparatus, product, or process disclosed, or represents that its use would not infringe privately owned rights. Reference herein to any specific commercial product, process, or service by its trade name, trademark, manufacturer, or otherwise, does not necessarily constitute or imply its endorsement, recommendation, or favoring by the United States Government or any agency thereof, or the Regents of the University of California. The views and opinions of authors expressed herein do not necessarily state or reflect those of the United States Government or any agency thereof or the Regents of the University of California.

UCRL-16362

un d. data

cy 2

UNIVERSITY OF CALIFORNIA

Lawrence Radiation Laboratory
Berkeley, California

Contract No. W-7405-eng-48

BRANCHING RATIOS IN K^+ MESON DECAY

Poh-shien Young

Ph.D. Thesis

September 15, 1965

for copy 2

UCRL-16362

UNIVERSITY OF CALIFORNIA
Lawrence Radiation Laboratory
Berkeley, California

AEC Contract No. W-7405-eng-48

August 17, 1966

ERRATA

TO: All recipients of UCRL-16362
FROM: Technical Information Division
Subject: UCRL-16362, "Branching Ratios in K^+ Meson Decay"

Please make the following corrections on subject report.

Page 45, line 6: Change $-C(\beta)$ to $-2C(\beta)$ *OK*

Page 67, last line in Table A-2 35 18 9 13.00 1.4
change to 165 83 42 6.76 3.8 *OK*

UCRL-16362

UNIVERSITY OF CALIFORNIA
Lawrence Radiation Laboratory
Berkeley, California

AEC Contract No. W-7405-eng-48

December 17, 1965

ERRATA

TO: All recipients of UCRL-16362. *done*
FROM: Technical Information Division.
Subject: Replace pages in report with attached.)
BRANCHING RATIOS IN K^+ MESON DECAY

BRANCHING RATIOS IN K^+ MESON DECAY

Contents

Abstract	iv
Chapters	
I Introduction	1
II Experimental Procedure	
1 Exposure and Processing of the D-Stack	8
2 Scanning Technique.	11
3 Identification of K^+ Decay Modes	15
4 Determination of Scanning Efficiency.	27
III Results	
1 Branching Ratios of the K^+ Decays.	32
2 Discussion of Results.	39
Acknowledgments.	42
Appendices	
I Calibration for Ionization Measurements.	43
II Energy Spectra of $K_{\mu 3}$ and τ^+	62
III Positrons in the Experiment.	65
IV π -Decays in Flight.	71
References	72

BRANCHING RATIOS IN K^+ MESON DECAY

Poh-shien Young

Lawrence Radiation Laboratory
University of California
Berkeley, California

September 15, 1965

ABSTRACT

A comprehensive study of the branching ratios in K^+ meson decay has been carried out by reviewing previous work and performing a new experiment. For this research a beam of 10^6 K^+ mesons was brought to rest in a volume of 14 cc within a large stack of nuclear research emulsion at the Lawrence Radiation Laboratory, Berkeley. The stack was designed so that the secondaries of the longest range could be followed to rest if the directions of their emission lie within certain cones. Some 700 K^+ decays for which each secondary was emitted in the selected cones were chosen as the sample for the experiment. The principal method for identifying the secondaries was following the track to rest, thus avoiding many sources of systematic error. Ionization measurements were used to resolve ambiguities. The overall efficiency for finding events was found to be higher than 95% and the relative efficiencies for the various modes were evaluated.

The corrected branching ratios for the $K_{\mu 2}$, $K_{\mu 3}$, $K_{\pi 2}$, τ , τ' , and $K_{e 3}$ were found to be 61.8 ± 2.9 , 5.4 ± 0.9 , 19.3 ± 1.6 , 6.0 ± 0.4 , 2.3 ± 0.6 , and 5.3 ± 0.9 respectively.

Chapter I Introduction

The branching ratios among different decay modes of K^+ meson have been measured several times in the past dozen years by different research groups either using the xenon bubble chamber^{1,2} or nuclear emulsion³⁻⁶. Discrepancies have been noticed not only between the emulsion data and the bubble chamber data, but also among the data obtained from similar detectors under different experimental conditions. The discrepancy between the $K_{\mu 2}/K_{\pi 2}$ ratio obtained by means of the bubble chamber^{1,2} and some of the early emulsion measurements^{3,4} has appeared so consistently that it has been considered evidence of a "shadow universe"⁷.

We have carried out our measurement of the branching ratios with nuclear research emulsion and improved techniques. Track following was employed on a scale never before undertaken. The stack size was the greatest ever used for this purpose. Better blob density calibration was made, and more uniform development was achieved than in previous experiments. In addition, several new methods for the reduction of bias and for calculating scanning efficiencies were introduced.

The detailed description of the experiment will be presented in the subsequent two chapters. It is appropriate to review here some of the previous experiments.

The various decay modes of K^+ meson were considered to be different species by earlier researchers⁸ who employed cosmic radiation as a source of heavy mesons and Wilson chambers or emulsion plates as detectors. Only in 1955 with the advent of the intense K^+ beams artificially produced in the Bevatron^{3,9} was the mass of these "different" mesons found to be the same. In addition to this, the mean lifetimes of the

mesons were found to be equal¹⁰⁻¹². The identity of a K^+ meson having various decay modes was thus established. This naturally led, in principle, to the conclusion that the branching ratios between the various decay modes must remain constant apart from statistical fluctuations, irrespective of the detection methods. Generally speaking, all branching ratio experiments have shown an agreement on the order of the frequencies of the major modes. However, the magnitude of individual branching ratios varied from one experiment to another. This variation could be attributed to the choice of a particular sample size and to the method of identifying secondaries. In reviewing previous work, these two factors should be considered of prime importance.

Our review will start with the two experiments performed separately in Berkeley by the Birge Group³ and Alexander et al.⁴ since they have been referred^{1,2,7} to as the most precise emulsion data for the K^+ branching ratios. A study of Birge's experiment indicates that their sample size was moderate because only 149 $K_{\mu 2}$ and 77 $K_{\pi 2}$ were found for the major modes. Furthermore, different batches of samples were used to find different decay modes and the overall efficiency for detecting a K^+ secondary was 85%. Track following, the most direct method, was employed in identifying 97 events while blob counting at the K^+ decay point was used to determine 185 events. Blob counting is advantageous because it is far less time consuming than track following. However, this advantage is outweighed by statistical and systematic errors. First of all, the observed blob density distributions of $K_{\mu 2}$ and $K_{\mu 3}$ overlap the $K_{\pi 2}$ distribution^{3,9}. This causes ambiguities when one tries to distinguish between events for which the measured blob densities of the secondaries lies within the overlapping regions.

Secondly, the statistical error involved in blob counting generally makes it difficult to define a precise residual range (or energy) by blob density alone [See Fig. A-2]. Thirdly, the blob density may vary with pellicle depths, with pellicles, or with both. The results of such variations could be serious in Birge's experiment even with a careful calibration because of the fact that the different batches of their stack were processed at different times and in some cases were made up from different manufacturer's batches of emulsion.

In Alexander's experiment⁴, both the stack and the sample size were larger, but the identification method was based almost entirely on blob counts and scattering measurements. In their method, which is similar to the ionization measurement employed in our experiment [See Section 3, Chapter II], the blob density B and the scattering angle (in terms of $p\beta c$) were measured on two selected segments of a track. The resultant six parameters B_1 , B_2 , $p_1\beta_1 c$, $p_2\beta_2 c$, ΔB , and $\Delta(p\beta c)$ were used to identify the track. Since more information can be deduced from the combined measurements than blob counting alone, this method reduces ambiguities in some cases. However, there remain the statistical and systematic errors which make this method still far less clear cut than the track following. The scanning efficiencies in Alexander's experiment were found to be about the same as in Birge's experiment: ~100% for τ and 85% for lightly ionizing tracks.

The next two experiments to be reviewed were performed in Berkeley by Roe et al.¹ and Shaklee et al.² by use of the 30 cm diameter xenon bubble chamber. Since faster scanning can be performed with bubble chamber pictures than with emulsion plates, these two groups were able to select larger samples (which accordingly reduced the statistical



fluctuations on their branching ratios): 6300 K^+ mesons for Roe and 10,500 for Shaklee. In Roe's experiment¹, two characteristics of a xenon bubble chamber were utilized to separate the various K^+ decay modes. These characteristics are the high efficiency for conversion of gamma rays from π^0 into electron pairs and the ease of recognition of electrons. Consequently $K_{\mu 2}$ can be separated from the other modes in the chamber simply by looking at the K^+ decay point because each $K_{\mu 2}$ event has a singly charged non-electron secondary and no electron pairs. However, this very advantage introduces ambiguities between $K_{\mu 3}$, τ' , and $K_{\pi 2}$. These ambiguities would be removed if track following were applicable. Nevertheless, this was not possible since the 24 cm range of the π^+ from $K_{\pi 2}$ is too great for it to be followed through in a chamber of 15-cm radius. In addition, the μ secondary from a π^+ decay at rest has a range of only 1.3 mm and hence cannot be reliably identified. [In standard emulsion, the characteristic μ range is 600 μ which can be easily recognized under a microscope]. Under such conditions, Roe et al. used a kinematic test to separate $K_{\pi 2}$ from other modes. Because of measurement errors and multiple scattering of the secondary it was found² that a true two-gamma $K_{\pi 2}$ did not have a 100% probability of passing the test while some of the $K_{\mu 3}$, $K_{e 3}$, and τ' events passed the test. The average scanning efficiencies in Roe's experiment were $(85 \pm 2)\%$ for electron pairs and $(89 \pm 2.5)\%$ for electron recognition.

According to Shaklee et al.,² one of the motivations² for their experiment was the fact that some of the previous experimental values of the branching ratios were in disagreement by an amount significantly more than the errors assigned. Their experiment was regarded as in-



dependent of Roe's experiment because a different sample of film and a significantly different method of analysis² were employed. Their results support fairly well Roe's results with the exception of the $K_{\pi 2}/K_{\mu 3}$ ratios². The disagreement was believed² to be due to a systematic error in Roe's calculation of the probability that a $K_{\pi 2}$ would pass the $K_{\pi 2}$ kinematical test. In Shaklee's analysis, the kinematical test was also used but with bias corrections based on the Monte Carlo Calculations. The probability for $K_{\pi 2}$, $K_{\mu 3}$, $K_{e 3}$ or τ' to pass the test (given that precisely two gammas convert in the chamber) was calculated by simulating measured decay modes through the Monte Carlo method. Their calculations led to a lower rate for $K_{\mu 3}$ and a higher rate for $K_{\pi 2}$ [See Table 3-5, Chapter III]. Our experimental ratios of $K_{\mu 3}$ and $K_{\pi 2}$ agree better with Roe's observation than Shaklee's. We are thus inclined to believe that the loss of some true $K_{\pi 2}$ events due to their failure in passing the kinematic test may have been compensated for by some $K_{\mu 3}$, $K_{e 3}$ or τ' events which passed the test. As Shaklee's experiment was done in the same xenon chamber with similar scanning procedures, there is no need to repeat our comments made in the preceding section. However, two points should be mentioned: a. The probability of a τ' being mistaken for $K_{e 3}$ was found to be $(7 \pm 2)\%$. (This introduced the so-called $K_{e 3} - \tau'$ ambiguity.) b. The $K_{\mu 2}$ branching ratio was not measured directly but evaluated by subtracting from unity the sum of the ratios measured for the other decay modes. (Because of the propagation and accumulation of errors involved in measuring individual decay, the indirect evaluation of a major mode like $K_{\mu 2}$ leaves large room for error.)

Based on the review of the previous experiments, the current

measurement of the K^+ branching ratios has been so designed as to satisfy two purposes: large sample size and clear-cut track identification. As described in Section 3, Chapter II, a large stack and three appropriate cones have been chosen in order to make it possible, in principle, to follow through the charged secondaries of all decay modes to their endings. The volume of cones constitutes 19% of the whole stack volume [See Table 2-1]. Thus no more than 19% of the K^+ decays contained in the scan volume were selected as the sample under this criterion. The reduction of the scan volume was compensated for by using an intense K^+ beam. By virtue of refinements made on the bevatron during the period between 1956 and 1963, the proton beam intensity was increased a hundredfold. We thus obtained about 4000 K^+ decays within a scan volume of $\sim 0.13 \text{ cm}^3$ in a 30-hour exposure period. Out of the 4000 K^+ decays some 700 were selected according to the cone criterion. Although a much larger scan volume (and thus a larger sample of K^+ decays) could have been extracted from the stack, we limited our sample to 700 because of the availability of scanner time.

Although track following was chosen as the principle method of identification, not all secondaries could be followed to their endings, irrespective of the stack design and the selection of cones. In addition, track following also has systematic errors although their effects are not as great as those associated with indirect methods. Therefore, special analyses were devised to correct for these errors, and range-ionization measurements were introduced as a supplementary method to identify tracks. The best available energy spectra of $K_{\mu 3}$ and τ' have been employed in the resolution of the K_{μ} events and the calculation of relative efficiencies [See Chapters II and III, and Appendix II]. In

order to check the effect on our results of uncertainties in these spectra, several varied spectra have been generated and the effect has been found to be negligible.

Generally speaking, the results of the current experiment agree better with bubble chamber data than with early emulsion measurements. We may, therefore, conclude that no basic discrepancy should exist in the branching ratios regardless whether bubble chamber or emulsion is used to perform an experiment.

The whole experiment with analysis is presented in two subsequent chapters. In Chapter II, experimental procedures, such as the scanning of the events, and the identification of secondaries, are described. Also included in the chapter are the treatments for the difficult events and the determination of the overall efficiency for the experiment. At the beginning of Chapter III, the observed branching ratios are calculated. Scanning bias and possible errors in track following are then discussed. This leads to the determination of the corrected branching ratios. The results are compared with the data cited and with some theoretical predictions.

Detailed calculations and reference curves are included in the four appendices. These materials are not only essential to the analysis carried out in the text but also useful for future reference.

Chapter II Experimental Procedure

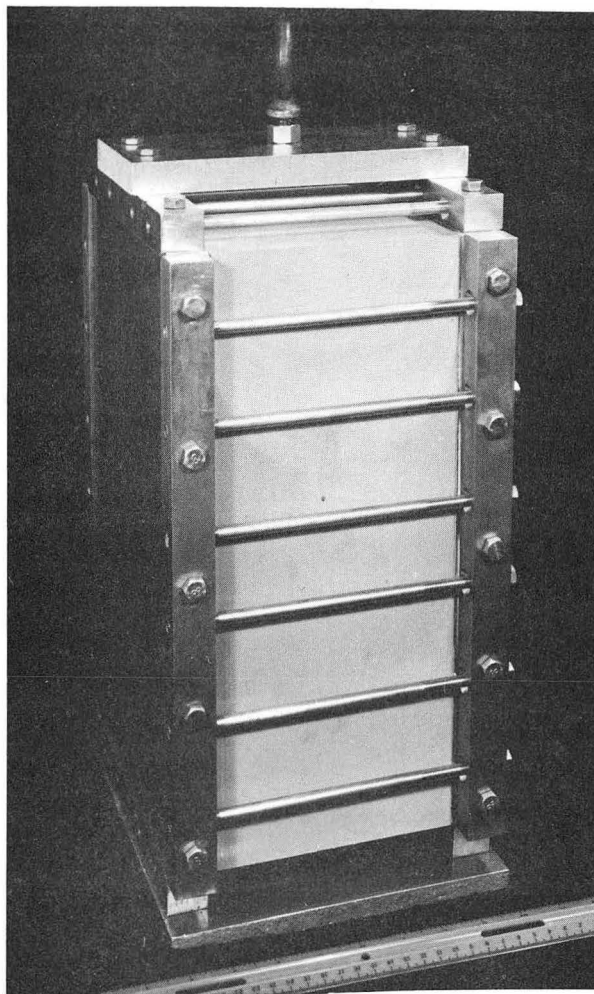
The experiment consists of four major parts: 1) Exposure of the D-stack, 2) Scanning for K-mesons, 3) Identification of decay modes, 4) Determination of scanning efficiency. These steps are described in some detail in the subsequent four sections.

Section 1 Exposure and Processing of the D-stack

The D-stack contains 250 Ilford K-5 emulsion pellicles, each 600 μ thick and 9" x 14" in area. The size of the stack was chosen so that a beam of K^+ mesons with a momentum of 130 MeV/c would come to rest and decay in the middle of the stack, and so that all the secondaries π^+ , μ^+ or e^+ within certain cones could be followed from K^+ decay point to termination.

The exposure of the stack to the K^+ meson beam took place in May 1963, at the Bevatron of the Lawrence Radiation Laboratory in Berkeley. Shown in Figs. 2-1 and 2-2 are a photograph of the D-stack and a diagram of the exposure arrangement, respectively. Fig. 2-2 is a schematic diagram in which the relative positions, but not the sizes, of the various components are shown. The stack was placed so that the K^+ beam was perpendicular to the surface of the pellicles and entered from the top of the stack (i.e. Plate No. D-250). The exposure area was about 5.3 cm x 2.5 cm, and approximately 10^6 K^+ mesons were admitted during an exposure period of 30 hours.

Immediately after exposure, the pellicles were separated and underwent the standard processes of grid printing, developing, and fixing. The grid printing provided the x-y coordinates of incident particles. The majority of the K^+ decays were found to have occurred



ZN-4969

Fig. 2-1 The D- Stack

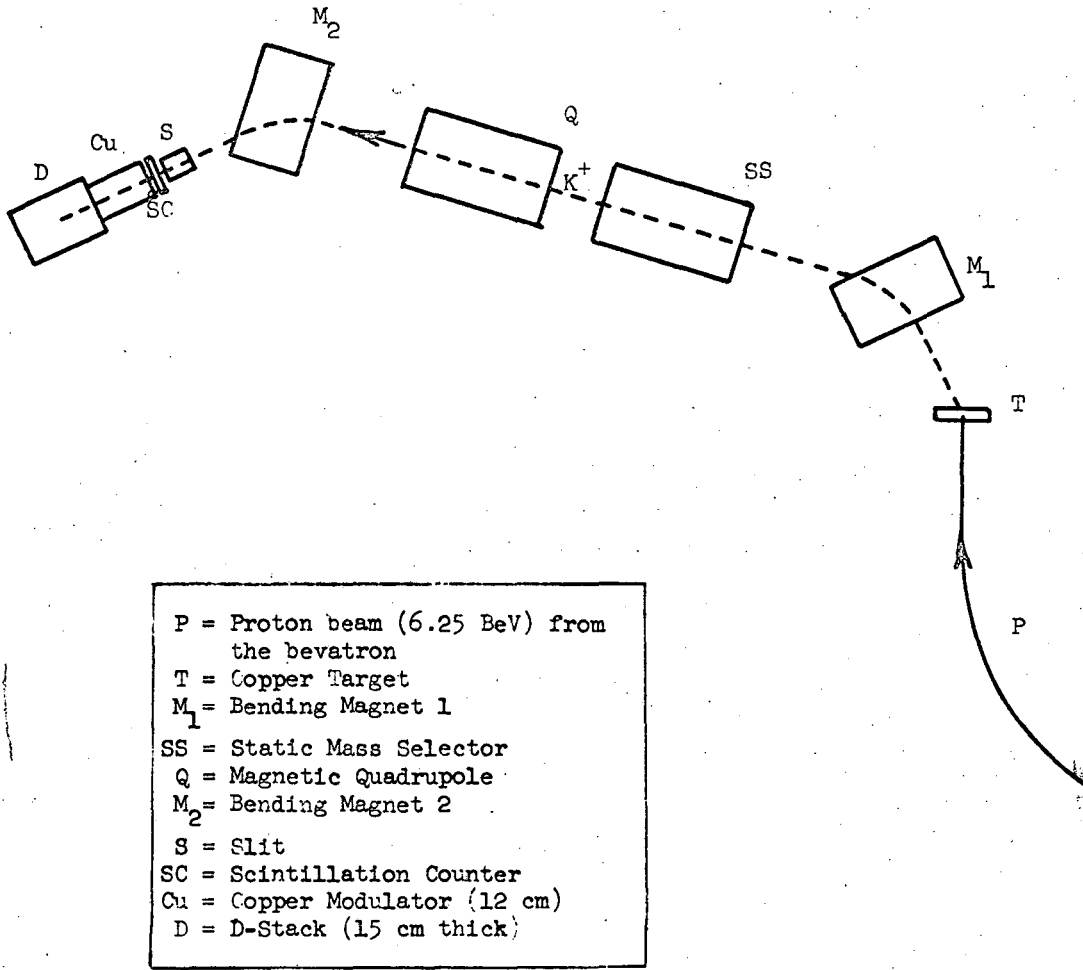


Fig. 2-2 Schematic Diagram of Exposure Setup

MU-36601

in 20 plates, i.e. in plates D-126 to D-145 inclusive. Therefore we may estimate that the 10^6 incoming K^+ mesons stopped in an appropriately located volume of 14 cm^3 .

Section 2 Scanning Technique

Great care has been exercised in the scanning work since it is extremely important in any branching ratio experiment. Before starting the scanning, two aspects were carefully considered: i) Choice of a suitable sample size, ii) Possibility of following various secondaries to rest.

Each scanner was given written instructions which were carefully prepared and contained all necessary details as to how to find the K^+ mesons and how to record the events. As the first step in scanning, every stopping track which entered the emulsion from the upper hemisphere was recorded during the first area scan even if, at that time, there was no secondary found associated with it. Any event whose primary looked like a possible K^+ but with no secondary found in the first scan was labeled No-Visible-Secondary or "N.V.S." events (to be discussed in detail in Section 4 of this chapter). Such events have been searched repeatedly for secondaries by different scanners, some of them having undergone up to seven rescans.

Since secondaries of the decay modes $K_{\mu 2}$, $K_{\mu 3}$, and $K_{\pi 2}$ may not stop in the stack unless they are emitted into certain cones, three cones have been specified for the selection of events. These specifications are listed in Table 2-1 and secondary ranges are listed in Table 2-2.

Table 2-1 Specification of Cones

Cones	ϕ^* (Goniometer)	$\tan \delta$ (Dip)	Purposes
A	$-24.5^\circ \leq \phi \leq 19.5^\circ$	$-0.361 \leq \tan \delta \leq 0.290$	All secondaries of $K_{\mu 2}$, $K_{\mu 3}$, $K_{\pi 2}$ can be followed to rest
A'	$-41.5^\circ \leq \phi \leq 31.5^\circ$	$-0.614 \leq \tan \delta \leq 0.474$	Secondaries of $K_{\pi 2}$ can be followed to rest
B	$148.5^\circ \leq \phi \leq 221.5^\circ$		

* Projected angles seen in microscope

Table 2-2 Ranges of Secondaries of Non-rare Decay Modes of K^+

Decay Modes	Q (MeV)	T or T_{\max} (K.E. in MeV)	R or R_{\max} (cm) (Range in standard emulsion)
$K_{\mu 2}$	388.1	152.5	21
$K_{\mu 3}$	253.1	134.1	18
$K_{\pi 2}$	219.2	108.6	12
τ	75.0	48.1	3.5
τ'	84.2	53.2	4
$K_{e 3}$	358.3	227.9	12 *

* Electron range is poorly defined ¹³ on individual basis because of radiative energy loss.

Cone A was defined so that all secondaries lying within this cone could be followed up to 23 cm which is greater than the range of the secondary of $K_{\mu 2}$ and thus greater than the secondary range of any decay mode. In order to supplement Cone A, Cone A' and Cone B were added shortly after scanning had started. Any secondary lying within Cone A' or Cone B could be followed at least up to 14 cm which is greater than the range of the secondary of $K_{\pi 2}$. Although $K_{\mu 2}$ and $K_{\mu 3}$ secondaries lying within Cone A' will sometimes not stop in the stack, the division of events between these two classes can be accomplished sufficiently well on the basis of the known $K_{\mu 3}$ matrix element and the observed number of $K_{\mu 3}$ events with shorter secondary ranges.

It is evident that K^+ tracks which stop near the top or bottom of the pellicle may not have secondaries that are observable if the secondary is directed towards the nearby surface. Thus, another criterion for a selected event was that the incident K^+ particles must stop within the middle two-thirds of the pellicle depth.

There were two types of record used for the scanning: scanner's notes and keysort cards. The scanner's notes were recorded directly on grid reproduction sheets (see Fig. 2-3). By specific notations, all the visible information about every K^+ meson found in the area was recorded. The information which was recorded is as follows: the grid location of each possible stopping K^+ , depth of the track ending (i.e. whether within, or not within, the middle two-thirds of the pellicle depth), the number of secondaries seen (i.e. whether a 1-prong, 3-prong or 0 prong event), a visual estimate of secondary ionization (i.e. whether near minimum or above minimum), and the goniometer angle for each 1-prong event. If a keysort card was made for the event, this

021 + 139	022 + 139	023 + 139
021 + 140	022 + 140	023 + 140
021 + 141	022 + 141	023 + 141
021 + 142	022 + 142	023 + 142
021 + 143	022 + 143	023 + 143

Fig. 2-3 Grid Reproduction Sheet

also was indicated on the grid reproduction sheet. For every event that satisfied certain criteria, the scanners were instructed to make a keysort card in order to provide a permanent record of the event.

These criteria were:

1. K^+ decay vertex must lie within middle two-thirds of the pellicle depth.
2. Secondary must lie within Cone A' or Cone B.

The first criterion was required for all stopping K^+ mesons with one or three prongs found at the decay point, while the second was required only for events with one near-minimum secondary. A sketch of the event was made and the goniometer and dip angles of the secondaries were recorded on the keysort card.

Section 3 Identification of K^+ Decay Modes

The ionizing secondaries from all decay modes of the K^+ meson can be only pions, muons or electrons. The most direct way to differentiate between these in emulsion is to follow the tracks to their endings and observe terminal behavior. In standard emulsion a μ particle from pion decay at rest has a characteristic range of about 600 microns before it comes to rest and decays into an electron and neutrinos. It is possible for positrons to disappear through annihilation in flight; otherwise, their paths at very low energy appear characteristically tortuous. Furthermore, we know that the ranges of the $K_{\pi 2}$ and $K_{\mu 2}$ charged secondaries are unique (21 cm for μ and 12 cm for π) because these are two-body decays. Since the range of the μ from $K_{\mu 3}$ decay can vary from 0 to 18 cm, the separation of $K_{\mu 3}$ and $K_{\mu 2}$ should present no difficulties if all secondaries could be followed to rest. An analogous statement



is applicable to the $K_{\pi 2}$ and τ' modes since the maximum range of the π^+ from τ' decay is 4 cm. The τ decay mode yields 3 above-minimum prongs and cannot be confused with any other common mode. From the above analysis, we may conclude that the branching ratios of the non-rare decay modes of K^+ could be easily determined if all charged secondaries could be followed to their endings. However, in practice, for one reason or another, not all secondaries could be followed to their endings in spite of the proper design of the D-stack and the appropriate choices of the cones. Hence ionization measurements and special analyses were also used as necessary to aid in identifying decay modes. An account of our process of identification using various methods is given below.

At the first stage over 300 of the one-prong events were followed either to their endings or as far as possible. All Cone A events were so treated. The remainder of the one-prong events were followed only up to 12 cm. From the range considerations (see Table 2-2) we know that any event with a secondary range greater than 12 cm could only be either $K_{\mu 2}$ or $K_{\mu 3}$. The 314 events belonging to this category were labeled 12-cm events. These are treated under K_{μ} events in Subsection (e).

When the first track following was done, we found that approximately 90 events had secondaries which could not be followed for 12 cm or to their endings. These secondaries were either lost or went out of the stack in less than 12 cm due to changes in their original path directions by scattering, or seemed to disappear in flight (D.I.F.), or produced stars in flight (S.I.F.). The S.I.F. events, D.I.F. events, lost or out of stack events, and $K_{e 3}$ events are treated in Subsections (a),



(b), (c) and (d), respectively. Also given in subsection (a) is a brief discussion of the use of ionization measurements.

(a) S.I.F. Events: This category contained 40 events of which 17 had stars at $D > 5$ cm. (D = the distance from K decay point to any particular point on the secondary.) Among all secondaries of K^+ decay, π is the only particle which is strongly interacting and capable of producing a star in flight. Therefore this category can contain only $K_{\pi 2}$ and τ' events. Furthermore as the maximum range of a π^+ from τ' decay is 4 cm, only 23 S.I.F. events can be candidates for both $K_{\pi 2}$ and τ' . To resolve these events, we first made use of the ionization method which is based on two definite relations: one of these relates blob density (in blobs/100 μ) to ionization (in MeV-gm/cm²) and the other relates ionization to residual range. By combining these two relations, one is able to obtain a calibration curve in which the blob density of a track in a particular medium can be expressed as a function of residual range. In Appendix I the procedure for obtaining the calibration curve for μ and π in the D-stack is elaborated. To illustrate the use of the curve, let us suppose that a star in flight is observed at 2.00 cm from the K^+ decay point and that we want to know whether the secondary is a π from $K_{\pi 2}$ or from τ' . Blobs are counted for at least 10 fields of view (equivalent to 1000 μ) to get blob densities at the K^+ decay point and at the star, say 19.1 ± 0.7 blobs/100 μ and 21.5 ± 1.3 blobs/100 μ , respectively. Assuming that the secondary has its maximum kinetic energy if it is from τ' , then we can get the following information from Fig. A-3 and Table 2-2:

Particles	Blob Density (blobs/100 μ)	
	At D = 0	At D = 2.00 cm
π from $K_{\pi 2}$	19.0	20.5
π from τ'	25.0	30.2

Comparing the above table with the measured blob densities, we see that the secondary is a π from $K_{\pi 2}$. In this way, all 23 S.I.F. events which had star at $D < 5$ were resolved. The resolution of all 40 S. I. F. events is tabulated below:

Table 2-3 Resolution of S.I.F. Events

No. of events	Identity	Method	Remarks
17	$K_{\pi 2}$	Range Measurement	Star at $D > 5$ cm
21	$K_{\pi 2}$	Ionization	Star at $D < 5$ cm
2	τ'	Ionization	Star at $D < 5$ cm

(b) D.I.F. Events: There were 11 events in this category as the result of the first track following. The primaries and secondaries of these 11 apparent D.I.F. events have been re-checked with great care by different scanners. As a result only one of them remains in the D.I.F. category. The secondary of this one remaining D.I.F. event has been refollowed and its scattering behavior indicates it is probably an e^+ . One of the 11 events is not a K decay. For 7 events the secondaries were scattered in such directions that they were not seen during the first following. Ionization measurements and further following showed that these are probably all K_{μ} events. A careful examination of the secondary ending of one event showed that it was an S.I.F. rather than a D.I.F. The secondary of the last event was refollowed with the result

that an error had been made during the original follow-through. This event was also an S.I.F. The original D.I.F. events have been classified as follows:

Table 2-4 Treatment of D.I.F. Events

No. of Events	Identity	Method	Remarks
4 3	K_{μ} (unambiguous) K_{μ} (probable)	Range measurement and ionization	To be treated in Subsection (e) (Two were followed to 12 cm in the second following)
2	$K_{\pi 2}$	Range measurement and ionization	One Star at $D = 5.68$ cm and the other at 6.03 cm (All were included in S.I.F.)
1	$K_{e 3}$ (probable)	Range measurement and ionization	
1	Not a K^+ decay	Recheck of the primary	The primary was a μ from a π -decay and the secondary was an e.

(c) Lost or out of Stack Events: 35 events were included in this class. Although the lost events have been rechecked very carefully there remain some whose secondaries still cannot be followed 12 cm or to their endings. Their identities have been resolved as tabulated below:



Table 2-5 Disposition of Lost or Out of Stack Events

No. of Events	Identity	Method	Remarks
7	K_{π^2} (unambiguous)	Ionization, range, and observation of behavior at end	
1	K_{π^2} (probable)		
20	K_{μ} (unambiguous)	Ionization and range	To be treated in subsection (e)
6	K_{μ} (probable)		
1	Unresolved		

(d) K_{e3} Events: There exist two possibilities by which an event originally classified as K_{e3} may not be a true K_{e3} : (i) the primary is a μ or (ii) an error made during the first track following led from the true secondary track to an e^{\pm} track. In order to minimize the possibility of errors being made in the identification of these events, two steps have been carried out -- all primaries were followed back and all secondaries were independently refollowed.

Although the exposure was arranged so that only the K^+ component of the beam would stop in the stack, K decays occurred upstream from the scan volume. In this case, the secondary would be a μ or π (which in turn will decay into μ). Therefore, we should not be surprised if some $\mu \rightarrow e$ events have been mistaken for $K \rightarrow e$ events. For this reason, we had all the primaries of the 62 original K_{e3} events rechecked. The result showed that 12 of these were $\mu \rightarrow e$ decays.

The second possibility for error stems from the fact that in all non-rare K^+ decay modes except K_{μ^2} and τ , at least one of the secondaries is a π^0 which decays into either two photons, one photon and one Dalitz pair (with branching ratio 1/80), or two Dalitz pairs (with branching ratio 2/80²). In other words, $\sim 30 \pi^0$ are produced per 100 K^+ decays.



This results in ~ 60 photons per $100 K^+$ decays. Assuming that the average energy of the photons from π^0 decay is ~ 100 MeV (67.5 MeV in π^0 rest frame), we notice that the corresponding mean free path for pair production in emulsion by these photons is 5.09 cm^{14} . This means that almost all photons from π^0 decay convert into electron pairs in the stack. Therefore, for every $100 K^+$ decays in the stack, $\sim 120 e^\pm$ tracks are produced. Almost all of these e^\pm tracks point generally back toward the scan volume which is very small compared with the whole stack. It is therefore estimated (details given in Appendix III) that, given a follow through error, there exists a probability of about 36% that one will be led to an electron (or positron) track. This reasoning demonstrates the necessity of refollowing all secondaries of the remaining K_{e3} events. The accomplishment of this task revealed that 14 of the original K_{e3} events were, in fact, so classified due to errors in the first follow through. The disposition of all events originally classified as K_{e3} is shown in Table 2-6.

Table 2-6 Resolution of Original K_{e3} Events

No. of Events	Identity	Method	Remarks
36	K_{e3}	Following and refollowing both primary and secondary	
12	K_μ	Following and refollowing both primary and secondary	To be treated in subsection (e) (All were followed to 12 cm in the second following)
2	$K_{\pi 2}$	Range and followthrough	One was included in S.I.F. (>5 cm) and the other in Lost Events.
12	$\mu \rightarrow e$	Following back primary	

(e) K_{μ} Events: From the discussion in the preceding subsections we have noticed that there are 359 K_{μ} events of which 314 are 12-cm events and 45 were labeled lost, out of stack, D.I.F. or K_{e3} events. The secondary of each of these was identified as a μ from either a range measurement or a combined range and ionization measurement. We still, however, needed to determine how many of them belong to the $K_{\mu3}$ mode. This was accomplished by use of the energy spectrum of the $K_{\mu3}$ and the number of $K_{\mu3}$ events in which the μ^+ was observed to decay at rest. The spectrum can be evaluated by integrating the square of the known matrix element over the possible final states. Given in Fig. A-4, Appendix II, is a normalized spectrum of the $K_{\mu3}$, dN/dT , as a function of the kinetic energy T . In emulsion research, the residual range, R , is subject to direct measurement. For this reason, we have converted dN/dT to dN/dR by use of Fig. A-2 (See Appendix I). The histogram of the range spectrum $dN/dR = F(R)$ is plotted as a function of R in Fig. 2-4. We may now proceed to describe our method of computing the expected number of $K_{\mu3}$ events whose secondaries were not followed to rest.

Consider a pure $K_{\mu3}$ sample of N events. Each secondary is to be followed for a distance $D (< R_{\max})$ if it does not decay at rest before that point. The expected number of decays at rest to be observed is then given by

$$N_{\mu3-d} = N \int_0^D F(R) dR \quad (2-1)$$

where $\int_0^{R_{\max}} F(R) dR = 1$ and R_{\max} = maximum residual range of a $K_{\mu3}$.
(See Table 2-2)

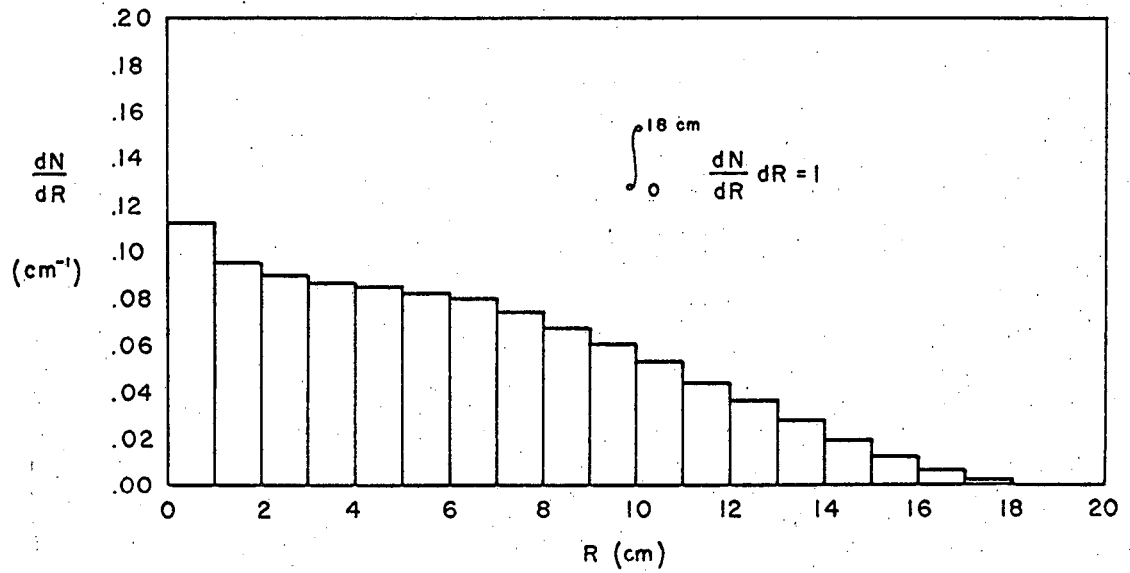


Fig. 2-4 Spectrum of $K_{\mu 3}$ as Function of Residual Range

MU-36590

Now consider a slightly more complicated case where the N events are separated in s groups, each containing Δn_i events ($i = 1, 2 \dots s$). Each secondary of one group is to be followed up to a particular distance D_i if it does not come to rest and decay before reaching that point. Treat each group in the same manner as before but assume different D_i 's. Then the number of events whose secondary decays can be seen is expected to be

$$N_{\mu 3-d} = \sum_{i=1}^s \Delta n_i \int_0^{D_i} F(R) dR, \quad (2-2)$$

and in the special case $\Delta n_i = 1$ for all i , we have

$$N_{\mu 3-d} = \sum_i \int_0^{D_i} F(R) dR \quad (2-3)$$

Here the set of D_i 's constitutes a hypothetical path length distribution.

Finally, consider the practical case with which we are faced. In this case we have $N = 465$ events, which total includes 359 K_{μ} events, and 106 $K_{\mu 3}$ and $K_{\mu 2}$ events for which the secondary was observed to decay at rest (35 $K_{\mu 3}$ and 71 $K_{\mu 2}$). We want to estimate how many of the K_{μ} events belong to the $K_{\mu 3}$ mode. Before applying Eq. (2-2) to this case, we first have to determine the potential path distribution, Δn_i , for this experiment. This can be done by considering the group of K_{μ} and $K_{\mu 2}$ events because almost all of those events belong to the $K_{\mu 2}$ mode. This argument is based on the theoretical range distribution of the $K_{\mu 3}$ mode and the experimental results. The distribution in Fig. 2-4 shows that only 10% of the whole $K_{\mu 3}$ spectrum can have residual range larger than 11 cm, but in our case we see that 96% of the K_{μ} events have been followed for more than 11 cm. Therefore the K_{μ} and $K_{\mu 2}$

events taken together furnish an empirical potential path distribution. Let this distribution be represented by the set Δm_i . We may conclude that

$$\Delta n_i = k \Delta m_i, \quad (2-4)$$

where k = normalization factor,

Δm_i = No. of secondaries followed for a distance between $D_i - \sigma/2$ and $D_i + \sigma/2$ without being observed to decay at rest.

By definition, we have

$$\Sigma \Delta n_i = N = N_{\mu} + N_{\mu 2-d} + N_{\mu 3-d}, \quad (2-5)$$

and

$$\Sigma \Delta m_i = N - N_{\mu 3-d}, \quad (2-6)$$

where N_{μ} = No. of K_{μ} events,

$N_{\mu 2-d}$ = No. of $K_{\mu 2}$ for which secondary was observed to decay at rest,

$N_{\mu 3-d}$ = No. of $K_{\mu 3}$ for which secondary was observed to decay at rest.

Notice that our experimental data give the following numbers

$$\left. \begin{aligned} N &= 465, \\ N_{\mu} &= 359, \\ N_{\mu 2-d} &= 71, \\ N_{\mu 3-d} &= 35. \end{aligned} \right\} \quad (2-7)$$

Inserting Eqs. (2-5) and (2-6) into (2-4), yields

$$\Delta n_i = \frac{N}{N - N_{\mu 3-d}} \Delta m_i. \quad (2-8)$$

If $N_{\mu 3}$ is the total number of $K_{\mu 3}$ events in the sample, then

$N_{\mu 3}/N$ is the probability that a given event in the sample be a $K_{\mu 3}$.

By substituting Eq. (2-8) into (2-2), we see that

$$N_{\mu 3-d} = \frac{N_{\mu 3}}{N} \left(\frac{N}{N-N_{\mu 3-d}} \right) \sum_{i=1}^s \Delta m_i \int_0^{D_i} F(R) dR,$$

or

$$N_{\mu 3-d} = \frac{N_{\mu 3}}{N-N_{\mu 3-d}} \left[\sum_{i=1}^{N_{\mu}} \int_0^{D_i} F(R) dR + \sum_{i=1}^{N_{\mu 2-d}} \int_0^{D_i=R_{\max}} F(R) dR \right] \quad (2-9)$$

for the case $\Delta m_i = 1$.

From the experimental data, we obtain

$$\sum_{i=1}^{N_{\mu}} \int_0^{D_i} F(R) dR = 325.7, \quad (2-10)$$

and

$$\sum_{i=1}^{N_{\mu 2-d}} \int_0^{D_i=R_{\max}} F(R) dR = N_{\mu 2-d} = 71 \quad (\text{since } \int_0^{R_{\max}} F(R) dR = 1) \quad (2-11)$$

If we substitute Eqs. (2-7), (2-10), and (2-11) into (2-9) and solve the result for $N_{\mu 3}$ we obtain

$$N_{\mu 3} = 37.9,$$

or

$$N_{\mu 3-d} + N'_{\mu 3} = 37.9,$$

whence

$$N'_{\mu 3} = 2.9. \quad (2-12)$$

Here $N'_{\mu 3}$ represents the number of $K_{\mu 3}$ for which the secondaries have not been followed to their decay points.

Eq. (2-12) indicates that the endings of about three $K_{\mu 3}$ events

were not observed because the decay secondary traveled farther than 12 cm, was lost or left stack.

Section 4 Determination of Scanning Efficiency

All track endings found during the original scan and classified as possible K's were searched for a secondary on at least two different occasions by the original scanner, provided no secondary was seen during the first search. The events for which no visible secondaries were found in any of these searches were labeled No-Visible-Secondary (N.V.S.) events. These have subsequently been investigated with great care in order to provide one of the two pieces of information upon which the evaluation of our scanning efficiency is based. The treatment of the N.V.S. events is discussed in Subsection (a) below. In Subsection (b) we will discuss the efficiency re-scan program. This furnished the second basis for efficiency evaluation.

(a) N.V.S. Events Program: Those N.V.S. endings contained within the middle $2/3$ of their respective pellicle depths were selected for further study and those N.V.S. endings not so contained were discarded at this stage. An extremely careful search for a secondary was made at each selected ending. If no secondary was found to be associated with an ending, then the primary was followed back to see if it belonged to the incoming K^+ beam. Finally, each residual N.V.S. event whose primary did belong to the beam was subjected to yet another rigorous search for a secondary.

The results of this program are listed below:

1. 1070 N.V.S. events were found to be contained in the middle $2/3$ of their respective pellicle depths,

2. Secondaries were ultimately observed for 382 out of the original 1070 N.V.S. events,
3. The primaries of 684 of the original N.V.S. events do not belong to the K^+ beam,
4. There remain only four endings whose primary appears to belong to the incoming K^+ beam but for which no secondary has yet been found.

From this result we may conclude that secondaries have eventually been seen for practically all of the genuine K^+ endings (in the middle 2/3) which were recorded during the original scan. All events with secondaries in the cones found during the course of the N.V.S. event program have been followed out and included in our sample.

(b) Efficiency Rescan Program: Some appropriately chosen parts of the original scan area have been rescanned independently by different scanners who were instructed to record (on grid reproduction sheets) every track ending coming from the upper hemisphere and lying in the middle 2/3 of the pellicle depth. No special effort was made to see secondaries during the efficiency rescan. The results were compared with the original scans to determine which endings in the same area were found in common, in the original scan only, or in the efficiency rescan only. Those events with endings seen only in the efficiency rescan have been put through the N.V.S. event program but not included in the branching ratio sample because the rescan area covers only a portion of the area originally scanned. The original scanning efficiency ϵ_0 is calculated in a conventional way. Let us assume that

N_T = "true" no. of events occurring in a scan area,

N_0 = number of events found from original scan in the area,

N_r = number of events found from rescan in the area,

and

N_c = number of events found in common.

Then the original and rescan efficiencies are given by

$$\left. \begin{aligned} \epsilon_o &= \frac{N_o}{N_T} , \\ \epsilon_r &= \frac{N_r}{N_T} . \end{aligned} \right\} \quad (2-13)$$

Since the original scan and rescan were done independently by different scanners, the probability for an event to be found in common is thus equal to

$$\epsilon_o \epsilon_r = \frac{N_o N_r}{N_T^2} \quad (2-14)$$

By definition of scanning efficiency, this quantity should be equal to N_c/N_T , i.e.

$$\frac{N_o N_r}{N_T^2} = \frac{N_c}{N_T} ,$$

or

$$N_T = \frac{N_o N_r}{N_c} . \quad (2-15)$$

From Eqs. (2-13) and (2-15) we can easily calculate ϵ_o . The results are tabulated in Table 2-8.

Table 2-8 Results of Efficiency of Rescan

Plate No.	N_c	N_o	N_r	Original Scan Efficiency
D-132	137	140	143	0.958
D-134	229	237	234	0.979
D-136	377	393	414	0.910
D-138	217	224	227	0.956
D-140	268	282	279	0.960

The total area covered in the original scan was 338 mm^2 and that covered in the efficiency rescan was 96 mm^2 . Although each individual plate efficiency was determined from a partial rescan area, we may assume that efficiency to be applicable to the entire plate because the original scan for each plate was carried out entirely by one particular scanner. Furthermore, the rescan area was distributed evenly over the entire original scan area. Therefore, by counting the K^+ decays found in the middle $2/3$ of each plate during the original scan, we are able to determine the overall efficiency ϵ for this experiment. In Table 2-9, we list all the relevant quantities.

Table 2-9 Determination of Efficiency for the Experiment

Plate No.	N_j		ϵ_j	N_j/ϵ_j
	1-Prong	3-Prong		
D-132	348	19	0.958	383.1
D-134	1248	72	0.979	1348.3
D-136	1019	58	0.910	1183.5
D-138	558	48	0.956	633.9
D-140	641	47	0.960	716.7

$$\Sigma N_j = N_{1 \text{ total}} + N_{3 \text{ total}} = 3814 + 244 = 4058$$

$$\Sigma(N_j/\epsilon_j) = 4266$$

$$\epsilon = \frac{N_j}{(N_j/\epsilon_j)} = 0.951$$

Notations: N_j = number of possible K^+ decays found in the middle 2/3 of the depth in Plate No. j.

ϵ = overall scanning efficiency for the experiment.

$N_{1 \text{ total}}$ = Total No. of 1-prong events found in the middle 2/3.

$N_{3 \text{ total}}$ = Total No. of 3-prong events found in the middle 2/3.

Chapter III Results

This chapter contains two sections. In the first section we will calculate the observed branching ratios and estimate the "true" branching ratios with efficiency correction. In the second section we will make general remarks on this experiment and compare our results with those obtained by other groups.

Section 1 Branching Ratios of the K^+ Decays

(a) Observed Branching Ratios: As mentioned in Section 2 of the previous chapter, the selection of each 1-prong event was based on the emission direction of the secondary. However, this selection rule cannot be applied directly to the τ events since these are 3-prong events. By assuming that K^+ decays isotropically, we can write down the following equation:

$$\frac{N_{1 \text{ cones}}}{N_{1 \text{ total}}} = \frac{N_{3 \text{ cones}}}{N_{3 \text{ total}}}, \quad (3-1)$$

where $N_{1 \text{ cones}}$ = No. of 1-prong events lying within the cones,

$N_{1 \text{ total}}$ = Total No. of 1-prong events found in the middle 2/3,

$N_{3 \text{ cones}}$ = No. of 3-prong events to be considered lying within the cones (namely, No. of τ events to be used in this branching ratio experiment),

and

$N_{3 \text{ total}}$ = Total No. of 3-prong events found in the middle 2/3.

To solve Eq. (3-1), we list the experimental data concerning the 1-prong events in Table 3-1. By combining the information listed in Tables 2-9 and 3-1, we are able to solve Eq. (3-1) for $N_{3 \text{ cones}}$ (or N_{τ}) as

$$N_3 \text{ cones} = 244 \times \frac{681}{3814} = 43.6, \quad (3-2)$$

or

$$N_\tau = 43.6. \quad (3-3)$$

Table 3-1 One-prong Events within the Cones

Decay Mode	Event Type					N_1 (No. of Events)
	Decay at Rest	12-cm Events or Lost or Out-stack	S.I.F. (< 5 cm) (> 5 cm)		D.I.F.	
$K_{\mu 2}$	71	356.1				427.1
$K_{\mu 3}$	35	2.9				37.9
$K_{\pi 2}$	85+3 [†]	8	19	19		134
τ'	15		2			17
$K_{e 3}$					1*	36
Misc.						27** + 1 ^{††}

$$N_1 \text{ cones} = \sum N_i = 681$$

* Probably $K_{e 3}$ [See Section (c), Appendix III]

** 1-prong events but not K^+ decay, included in N_1 cones because the value of N_1 listed in Table 2-8 refers to No. of 1-prong events found in the first area scan, of which some primaries may not be K^+ after further investigation.

† Of shorter ranges than should be, to be investigated further.

†† Unresolved events.



With the value of N_{τ} evaluated, we can calculate the observed branching ratios in K^+ meson decay. These are listed in Table 3-2.

Table 3-2 Observed Branching Ratios in K^+ Decay

Decay Mode	N_i (No. of i Events)	r_i (Branching Ratio)
$K_{\mu 2}$	427.1	61.31%
$K_{\mu 3}$	37.9	5.44%
$K_{\pi 2}$	134	19.24%
τ	43.6	6.26%
τ'	17	2.44%
$K_{e 3}$	37	5.31%
$\Sigma N_i = 696.6$		$\Sigma r_i = 100.00\%$

(b) Corrected Branching Ratios: Two items need to be considered in making corrections to the observed branching ratios listed in Table 3-2. The first one is related to the different efficiencies for finding examples of different K^+ decay modes. (Let us call them "relative efficiencies".) The second one involves possible errors in following secondaries. It is convenient to deal with the second item first because the discussion requires only a short paragraph.

In Appendix III, we have shown that the relative probability of a follow-through error, if any, leading to an e^{\pm} track as opposed to a μ or π track was about 36%. For this reason, we had all the original $K_{e 3}$ events refollowed independently. This demonstrated that fourteen of these events were not $K_{e 3}$. [See Section 3, Chapter II.] The total number of possible errors in the first following is then estimated to be $14/0.36 = 39$. In other words, there could be possibly 25 events of



which the secondaries might have led to a wrong π or μ track in the first systematic following. This number, compared with some 650 events of all decay modes except the K_{e3} , is so small that there is no need for a refollow of each K_{μ} or K_{π} event. In other words, there is no need for a correction in this respect for the measured branching ratios.

The difference in the relative efficiencies for different K^+ decay modes stems from the fact that each mode has a different energy spectrum which in turn leads to different spectra as functions of blob density. We estimate that a π track with kinetic energy less than 25 MeV (corresponding to ionization greater than 38.64 blobs/100 μ in the D-stack) can probably not be missed. In other words, we assume any secondary with ionization equal to or larger than 38.64 blobs/100 μ can be observed with efficiency 100%. For any secondary with ionization lower than 38.64 blobs/100 μ the efficiency will decrease with no definite relationship known to us. As the simplest approximation, we assume that the relationship is linear i.e., the efficiency ϵ_i can be expressed as a linear function of blob density B_i as follows:

$$\epsilon_i = \begin{cases} 1 - m (B_{25} - B_i) & \text{for } B_i < B_{25}, \\ 1 & \text{for } B_i \geq B_{25}. \end{cases} \quad (3-4)$$

where m is to be determined, B_i refers to a particular blob density corresponding to ϵ_i , and B_{25} represents the blob density corresponding to a 25 MeV pion. The meaning of ϵ_i is defined by the following equation:

$$\frac{N_i}{\epsilon_i} = N_i', \quad (3-5)$$

where N_i = observed number of events belonging to the i -th decay mode

and N_i' = true number of events belonging to the i -th mode.

Since the $K_{\mu 2}$ and $K_{\pi 2}$ secondaries have unique energies, we can apply Eqs. (3-4) and (3-5) directly to these 2 modes to obtain: [See Appendix I for the value of $B_{\mu 2}$ and $B_{\pi 2}$]

$$\epsilon_{\mu 2} = 1 - m (B_{25} - B_{\mu 2}) = 1 - 21.44 m, \quad (3-6)$$

$$\frac{N_{\mu 2}}{\epsilon_{\mu 2}} = N'_{\mu 2}, \quad (3-7)$$

$$\epsilon_{\pi 2} = 1 - m (B_{25} - B_{\pi 2}) = 1 - 18.45 m, \quad (3-8)$$

and

$$\frac{N_{\pi 2}}{\epsilon_{\pi 2}} = N'_{\pi 2} \quad (3-9)$$

The $K_{\mu 3}$, $K_{e 3}$ and τ' modes have continuous spectra. Thus, for these modes we must define their mean efficiencies as follows:

$$\bar{\epsilon}_{\mu 3} = \int_{B_{\min}}^{B_{25}} [1 - m (B_{25} - B)] \frac{dN}{dB} dB + \int_{B_{25}}^{B_{\max}} \frac{dN}{dB} dB, \quad (3-10)$$

$$\frac{N_{\mu 3}}{\bar{\epsilon}_{\mu 3}} = N'_{\mu 3}, \quad (3-11)$$

$$\bar{\epsilon}_{e 3} = \int_{B_{\min}}^{B_{\max}} [1 - m (B_{25} - B)] \frac{dN}{dB} dB \quad (\text{since } B_{\max} < B_{25}), \quad (3-12)$$

$$\frac{N_{e 3}}{\bar{\epsilon}_{e 3}} = N'_{e 3} \quad (3-13)$$

$$\bar{\epsilon}_{\tau'} = \int_{B_{\min}}^{B_{25}} [1-m(B_{25} - B)] \frac{dN}{dB} dB + \int_{B_{25}}^{B_{\max}} \frac{dN}{dB} dB, \quad (3-14)$$

and

$$\frac{N_{\tau'}}{\bar{\epsilon}_{\tau'}} = N'_{\tau'}, \quad (3-15)$$

where $\frac{dN}{dB} dB$ = number of events whose secondaries have a blob density lying between B and $B + dB$ at K^+ decay point.

As the efficiency for a 3-prong event was found to be approximately 100%, a simpler equation can be written down for the τ event:

$$N_{\tau} = N'_{\tau}. \quad (3-16)$$

By the definition of the overall scanning efficiency ϵ for the experiment [See Table 2-8], we may relate ϵ to different ϵ_i by the following equation:

$$\frac{\sum N_i}{\epsilon} = \sum N'_i = \frac{N_{\mu 2}}{\epsilon_{\mu 2}} + \frac{N_{\mu 3}}{\epsilon_{\mu 3}} + \frac{N_{\pi 2}}{\epsilon_{\pi 2}} + N_{\tau} + \frac{N_{\tau'}}{\epsilon_{\tau'}} + \frac{N_{e 3}}{\epsilon_{e 3}} \quad (3-17)$$

The corrected branching ratios are then defined by:

$$r'_i = N'_i / (\sum N'_i). \quad (3-18)$$

To solve Eqs. (3-17) and (3-18), we first have to calculate $\bar{\epsilon}_{\mu 3}$, $\bar{\epsilon}_{e 3}$, $\bar{\epsilon}_{\tau'}$. Note that

$$\frac{dN}{dB} dB = \frac{dN}{dT} \frac{dT}{dB} dB, \quad (3-19)$$

which can be evaluated for $K_{\mu 3}$ and τ' by use of Figs. A-3, A-4, and A-5



in Appendice I and II. For the calculation of $\bar{\epsilon}_{e3}$, see Section (a), Appendix III. The results of these calculations are

$$\left. \begin{aligned} \bar{\epsilon}_{\mu 3} &= 1 - 13.99 \text{ m,} \\ \bar{\epsilon}_{\tau 1} &= 1 - 2.55 \text{ m,} \\ \bar{\epsilon}_{e3} &= 1 - 20.83 \text{ m.} \end{aligned} \right\} \quad (3-20)$$

By substituting Eqs. (3-6), (3-8), (3-20), into (3-17) and using Tables 2-8 and 3-2 for the values of ϵ and N_1 , we obtain:

$$\begin{aligned} \frac{696.6}{0.951} &= \frac{427.1}{1-21.44\text{m}} + \frac{37.9}{1-13.99\text{m}} + \frac{134}{1-18.45\text{m}} + 43.6 \\ &+ \frac{17}{1-2.55\text{m}} + \frac{37}{1-20.83\text{m}}. \end{aligned} \quad (3-21)$$

Equation (3-21) has a total of five roots, of which the four positive ones below 10 are found:

$$\left. \begin{aligned} m_1 &= 0.002581, \\ .0506 &< m_2 < 0.0507, \\ .0707 &< m_3 < 0.0708, \\ .038 &< m_4 < 0.39. \end{aligned} \right\} \quad (3-22)$$

Among the four values, m_1 is the only acceptable one. The others lead to unreasonably small relative efficiencies. Once m_1 is accepted as the root we can easily calculate ϵ_1 or $\bar{\epsilon}_1$, N_1' and r_1' by use of equations (3-6), (3-7), (3-8), (3-9), (3-11), (3-13), (3-20). The results are listed in Table 3-3.

Table 3-3 Efficiencies and Corrected Branching Ratios

Decay Mode	ϵ_i Relative Efficiency	N_i^* ("True" No.)	r_i' Corrected Branching Ratio %
$K_{\mu 2}$	94.46%	452.15 \pm 21.26	61.75 \pm 2.90
$K_{\mu 3}$	96.39%	39.32 \pm 6.27	5.37 \pm 0.86
$K_{\pi 2}$	95.03%	141.01 \pm 11.88	19.26 \pm 1.62
τ	100.00%	43.60 \pm 2.79	5.95 \pm 0.38
τ'	99.34%	17.11 \pm 4.14	2.34 \pm 0.57
$K_{e 3}$	94.62%	39.10 \pm 6.25	5.34 \pm 0.85
		$\Sigma N_i' = 732.29$	$\Sigma r_i' = 100.0$
<p>* $\Delta N_i' = \sqrt{N_i'}$ for all decay modes except τ</p> <p>$\Delta N_{\tau}' = \sqrt{N_{\tau}' \text{ total}} \times (681/3814)$ [See Eq. (3-2)]</p>			

Section 2 Discussion of Results

(a) Comments: (i) As the majority of the events in this experiment were identified by the track following and all but 1 of the 11 D.I.F. events were resolved, practically no ambiguity exists between K_{μ} and K_{π} events, between $K_{\mu 2}$ and $K_{\mu 3}$ events, or between τ' and $K_{\pi 2}$ events. Listed in Table 3-4 is the summary on the identification of the events.



Table 3-4 Identification Methods Used in the Experiment

Category	Number of Events Identified		Total
	Track Following	Ionization Measurement or Other Method	
$K_{\mu 2}$ and $K_{\pi 2}$	515.1	46 (10 original D.I.F. 36 Lost or Out Stack)	561.1
$K_{\mu 3}$	35	2.9	37.9
τ	43.6		43.6
τ'	15	2	17
$K_{e 3}$	36	1 (Original D.I.F.)	37

(ii) Since both the overall and relative efficiencies were found to be sufficiently high (See Tables 2-8 and 3-3), there could only be a very few possible K^+ primaries and secondaries within the scan volume still unobserved.

(iii) Although the estimate made in Appendix III for the total number of e^{\pm} track produced around the scan volume was a rough approximation, it has provided for the first time a rational basis to carry out the calculation of possible errors in the first track following. This estimate, combined with the successful handling of the original $K_{e 3}$ events, has led to the conclusion that only negligible correction in this respect was needed for the branching ratios observed in the experiment.

(b) Comparison: We list five sets of the branching ratios measured by different groups in Table 3-5.



Table 3-5 Branching Ratios (%) in K^+ Decay

Measured by Different Groups

Decay Mode	Emulsion			Xenon Bubble Chamber	
	Birge ³ (1956)	Alexander ⁴ (1957)	Young (1965)	Roe ¹ (1961)	Shaklee ² (1964)
$K_{\mu 2}$	58.5 ± 3.0	56.9 ± 2.6	61.8 ± 2.9	64.2 ± 1.3	63.0 ± 0.8
$K_{\mu 3}$	2.8 ± 1.0	5.9 ± 1.3	5.4 ± 0.9	4.8 ± 0.6	3.0 ± 0.5
$K_{\pi 2}$	27.7 ± 2.7	23.2 ± 2.2	19.3 ± 1.6	18.6 ± 0.9	22.4 ± 0.8
τ	5.6 ± 0.4	6.8 ± 0.4	6.0 ± 0.4	5.7 ± 0.3	5.1 ± 0.2
τ'	2.1 ± 0.5	2.2 ± 0.4	2.3 ± 0.6	1.7 ± 0.2	1.8 ± 0.2
$K_{e 3}$	3.2 ± 1.3	5.1 ± 1.3	5.3 ± 0.9	5.0 ± 0.5	4.7 ± 0.3

Generally speaking, our results (especially for the major modes $K_{\mu 2}$ and $K_{\pi 2}$) agree better with the bubble chamber data than the early emulsion data. For this reason, we think that basically no discrepancy in the branching ratios should exist regardless whether nuclear research emulsion or bubble chamber is used to perform the experiment.

Since the value of some branching ratios of K^+ meson have been predicted by some theoreticians^{2, 15-17}, it may be interesting to compare our results with some of the predicted values. The comparison is tabulated in the table below

Table 3-6 Our K^+ Branching Ratios Compared with Predicted Values

Branching ratios	Measured value	Predicted value	Underlying theory
$K_{\mu 2}$	0.618 ± 0.029	0.677 ± 0.011	Universality ^{2,15}
$K_{\mu 3}/K_{e 3}$	1.00 ± 0.23	0.69	S-wave $K-\pi$ resonance ¹⁶
		0.64	P-wave $K-\pi$ resonance ¹⁶
τ'/τ	0.39 ± 0.10	0.325	$\Delta I = 1/2$ rule ¹⁷



ACKNOWLEDGMENTS

I should like to express my deep gratitude to Professor Walter H. Barkas and Dr. W. Zack Osborne for their guidance and advice throughout the experiment and analysis. The help and suggestions of Dr. Harry H. Heckman are greatly appreciated. I have benefited considerably from my association with Miss Frances M. Smith, Mr. Jack W. Patrick, and Dr. Douglas E. Greiner.

Sincere thanks to Miss Ernestine E. Beleal for her invaluable contribution in many phases of the project.

I also wish to thank the data analysts in the Barkas Physics Research Group for their excellent work. In particular, I wish to acknowledge Mrs. Marilyn A. Mollin and Mr. Robert E. Trankle for their assistance in resolving ambiguous events. I am also thankful to Mrs. Janice Dickson for her patient help in administrative work.

I am indebted to my wife Yung-hui for her help and encouragement throughout my graduate years. Without her I could never reach my long cherished goal.

This work was done under the auspices of the U. S. Atomic Energy Commission.

131

Appendix I Calibration for Ionization Measurements

The calibration of ionization in terms of grain density or blob density was carried out with respect to different depths in a plate, different plates in the stack, different particles, and different energies. Although the blob density is different from grain density, the difference is not large in our cases where grain densities concerned are lower than 50 grains per 100 μ . Since blob density is the quantity we have measured, it is employed in this work as an ionization parameter.

(a) Blob Density with Respect to Different Depths and Different

Plates: The secondaries of ten known $K_{\pi 2}$ and ten known $K_{\mu 2}$ were so chosen that their origins were distributed over ten plates: from D-132 to D-141. The ionization along each secondary from the point of its origin was measured in terms of blob densities for a path length equivalent to a thickness of 3 plates (or about a distance of 2 mm). The blob densities were first averaged over the three portions of each plate (i.e., upper, middle, and lower portions) and then over each whole plate. As the secondaries of the $K_{\pi 2}$ and $K_{\mu 2}$ modes have unique energies and the loss of energy at such energies along a path of 2 mm in standard emulsion is negligible, the secondaries of each category can be considered as two monoenergetic entities which should yield two constant ionizations in a 2 mm path. Our results demonstrated that the variations with respect to depths of each plate were all smaller than ± 1 blob/100 μ (See Fig. A-1) and those due to different plates were even smaller.

(b) Kinetic Energy as a Function of Residual Range R: As it is the residual range R, (rather than kinetic energy T or velocity β)

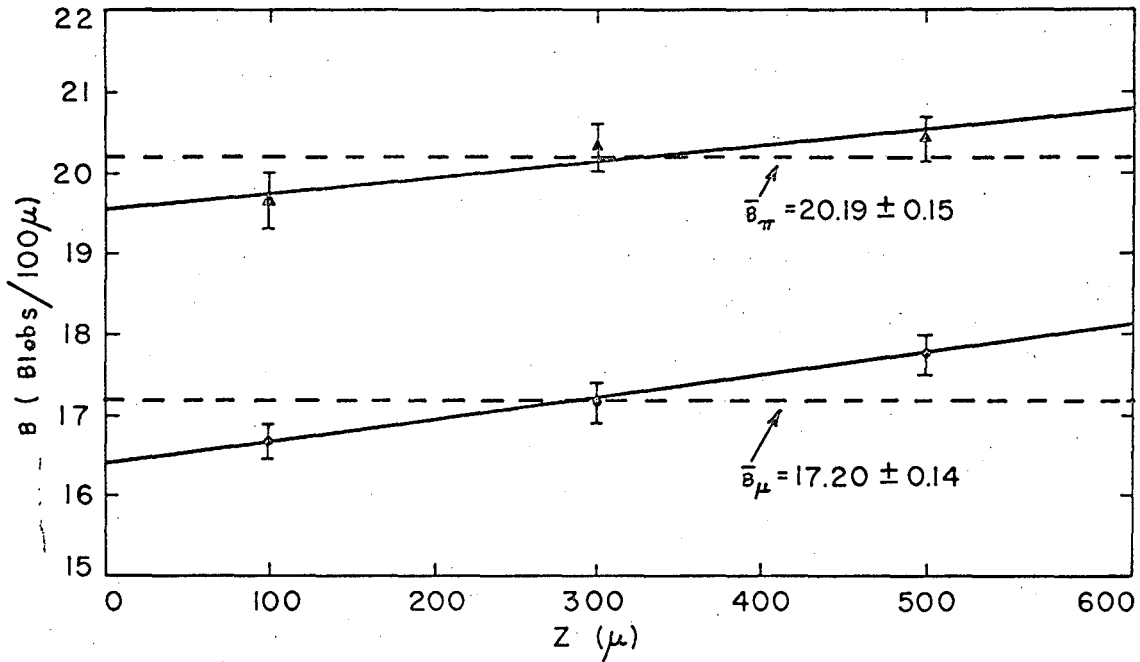


Fig. A-1 Blob Density as Function of Pellicle Depth
($Z = 0$ at Bottom)

which can be measured directly in emulsion, it is more convenient to express kinetic energy as a function of R. For this reason, we have used the following equations^{18,19} to calculate different i and R_p with different β and list the results in Table A-1.

$$i = \frac{2\pi r_0^2 m_e c^2 (n/\rho)}{\beta^2} \left[\ln \left(\frac{2m_e c^2 \beta^2 \gamma^2}{I} \right)^2 - 2\beta^2 - 2C(\beta) \right] \quad (\text{MeV-cm}^2/\text{gm}), \quad (\text{A-1})$$

and

$$R_p(T_p) = 0.00144 + \int_1^{T_p} \frac{dT_p}{i\rho} \quad (\text{cm}), \quad (\text{A-2})$$

where C(β) = Density correction term for standard emulsion,¹⁹

i = Total energy loss of a singly charged heavy particle,

$$2\pi r_0^2 m_e c^2 n = 0.2663 \text{ MeV/cm}$$

ρ = 3.815 gm/cc (density of standard emulsion),

I = 331 eV (mean excitation energy for standard emulsion),¹⁸

T_p = K.E. of a proton.

The residual range of a π or μ at the same β is related to R_p

by

$$\frac{R_\pi(\beta)}{R_p(\beta)} = \frac{m_\pi}{m_p},$$

or

$$\frac{R_\mu(\beta)}{R_p(\beta)} = \frac{m_\mu}{m_p}.$$

Similar expressions exist for T_π and T_μ, i.e.,



$$\frac{T_{\pi}}{T_p} = \frac{m_{\pi}}{m_p},$$

and

$$\frac{T_{\mu}}{T_p} = \frac{m_{\mu}}{m_p}.$$

The two curves plotted in Fig. A-2 and the various values of T, R and i listed in Table A-1 are the results of the above calculations.

It is appropriate to make some remarks on the value of I used in the above calculation. The exact value of the mean excitation energy for standard emulsion is at present uncertain. The old figure¹⁸ of 331 eV was employed in the calculation of i although there is recent evidence²⁰ that the best value of I is somewhat lower. The range and energy loss rate are, however, insensitive to I and the old value may be justified by noting that the range table (Table A-1) gives correctly the ranges of the $K_{\pi 2}$ and $K_{\mu 2}$ secondaries, which were measured incidental to this experiment.

(c) Blob Density B as a Function of Residual Range R. The blob density of secondary tracks at different R's from known $K_{\mu 2}$ and $K_{\pi 2}$ events have been measured. The experimental data are plotted in Fig. A-3 with an empirical calibration curve drawn to fit them. The curve has been used as the basis for the ionization measurements mentioned in Chapter II.

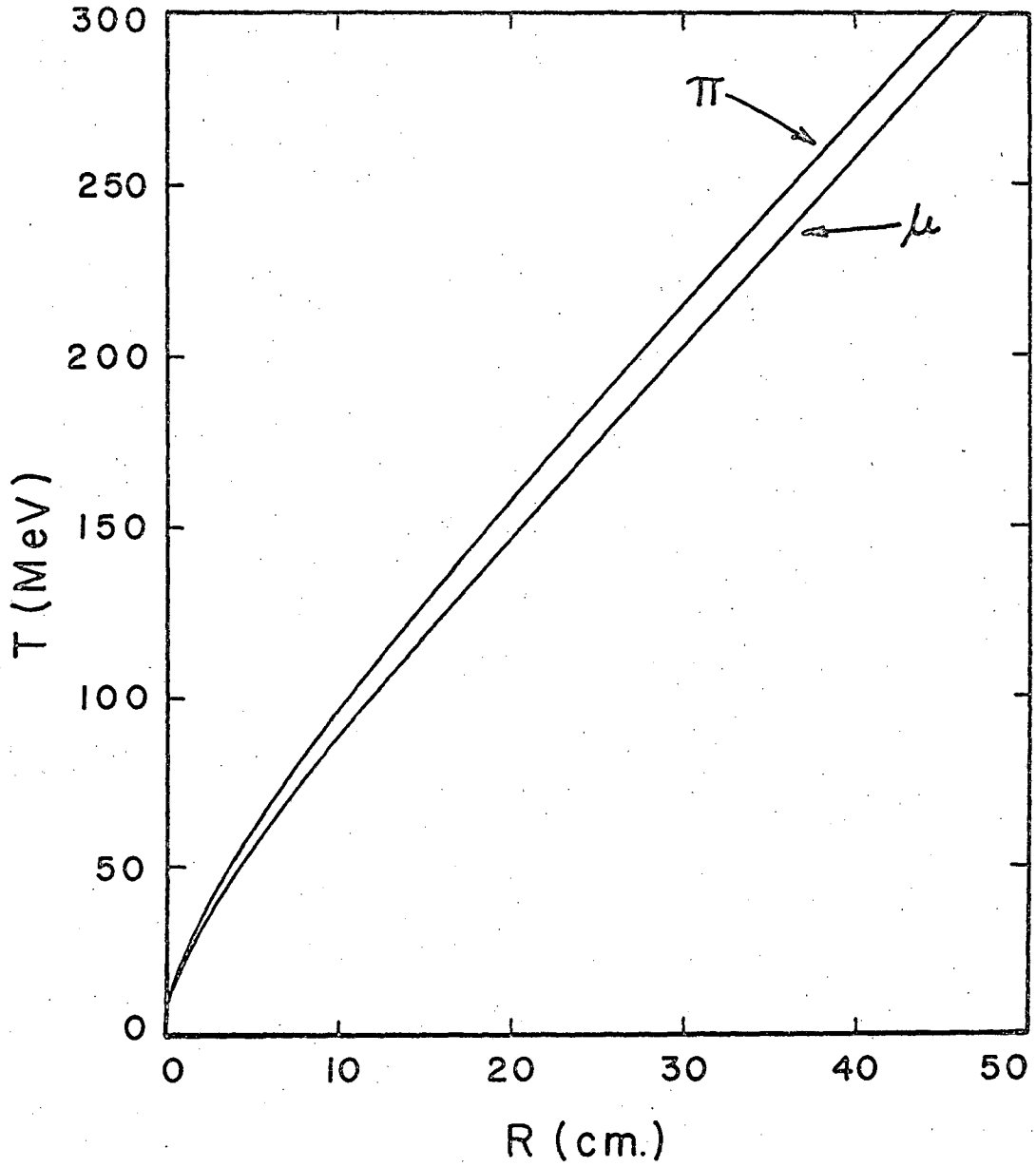


Fig. A-2 Kinetic Energy as Function of Residual Range for π and μ .

MU-36595

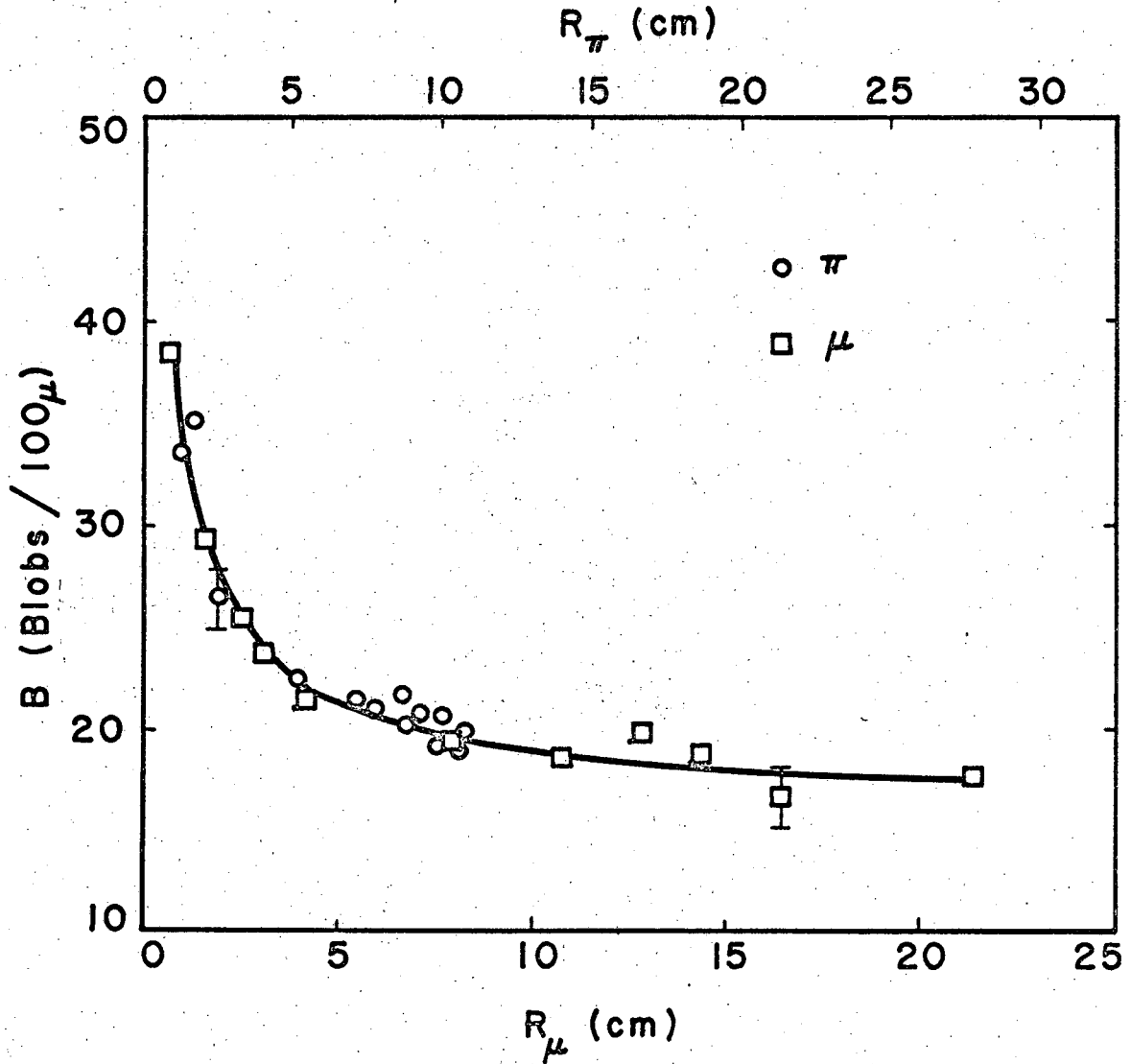


Fig. A-3 Blob Density as Function of Residual Range of μ and π

Table A-1 K. E., Residual Range, and Total Ionization
of p, π and μ

β (v/c)	T (MeV)			R (cm)			i $\left[\frac{\text{MeV-cm}^2}{\text{gm}} \right]$
	p	π	μ	p	π	μ	
0.4091447	90.000	13.390	10.135	2.600	0.387	0.293	5.0014235
0.4188535	95.000	14.134	10.698	2.867	0.427	0.323	4.8206049
0.4282070	100.000	14.878	11.261	3.143	0.468	0.354	4.6558811
0.4372306	105.000	15.622	11.824	3.430	0.510	0.386	4.5051665
0.4459467	110.000	16.366	12.387	3.725	0.554	0.419	4.3667244
0.4543754	115.000	17.110	12.950	4.030	0.600	0.454	4.2390971
0.4625345	120.000	17.854	13.514	4.343	0.646	0.489	4.1210515
0.4704403	125.000	18.598	14.077	4.665	0.694	0.525	4.0115369
0.4781073	130.000	19.342	14.640	4.996	0.743	0.563	3.9096526
0.4855489	135.000	20.086	15.203	5.336	0.794	0.601	3.8146216
0.4927772	140.000	20.830	15.766	5.683	0.846	0.640	3.7257704
0.4998032	145.000	21.574	16.329	6.039	0.899	0.680	3.6425111
0.5066372	150.000	22.317	16.892	6.403	0.953	0.721	3.5643294
0.5132885	155.000	23.061	17.455	6.774	1.008	0.763	3.4907726
0.5197658	160.000	23.805	18.018	7.154	1.064	0.806	3.4214410
0.5260771	165.000	24.549	18.581	7.540	1.122	0.849	3.3559799
0.5322299	170.000	25.293	19.144	7.935	1.181	0.894	3.2940736
0.5382310	175.000	26.037	19.707	8.336	1.240	0.939	3.2354399
0.5440869	180.000	26.781	20.270	8.745	1.301	0.985	3.1798269
0.5498036	185.000	27.525	20.833	9.160	1.363	1.032	3.1270068
0.5553869	190.000	28.269	21.396	9.583	1.426	1.079	3.0767753
0.5608419	195.000	29.013	21.960	10.012	1.490	1.127	3.0289474
0.5661737	200.000	29.757	22.523	10.448	1.554	1.177	2.9833557
0.5713869	205.000	30.500	23.086	10.891	1.620	1.226	2.9398476
0.5764859	210.000	31.244	23.649	11.340	1.687	1.277	2.8982848
0.5814749	215.000	31.988	24.212	11.795	1.755	1.328	2.8585405
0.5863577	220.000	32.732	24.775	12.256	1.824	1.380	2.8204973
0.5911382	225.000	33.476	25.338	12.724	1.893	1.433	2.7840551
0.5959199	230.000	34.220	25.901	13.198	1.964	1.486	2.7491104
0.6004059	235.000	34.964	26.464	13.677	2.035	1.540	2.7155761
0.6048997	240.000	35.708	27.027	14.163	2.107	1.595	2.6833692
0.6093040	245.000	36.452	27.590	14.654	2.180	1.650	2.6524140
0.6136219	250.000	37.196	28.153	15.151	2.254	1.706	2.6226394
0.6178560	255.000	37.940	28.716	15.654	2.329	1.763	2.5939819
0.6220089	260.000	38.684	29.279	16.162	2.405	1.820	2.5663793
0.6260831	265.000	39.427	29.842	16.675	2.481	1.878	2.5397763
0.6300809	270.000	40.171	30.406	17.194	2.558	1.936	2.5141205
0.6340047	275.000	40.915	30.969	17.717	2.636	1.995	2.4893634
0.6378566	280.000	41.659	31.532	18.247	2.715	2.055	2.4654595
0.6416387	285.000	42.403	32.095	18.781	2.794	2.115	2.4423667
0.6453528	290.000	43.147	32.658	19.320	2.874	2.176	2.4200454
0.6490011	295.000	43.891	33.221	19.864	2.955	2.237	2.3984586
0.6525852	300.000	44.635	33.784	20.413	3.037	2.299	2.3775717
0.6561069	305.000	45.379	34.347	20.966	3.119	2.361	2.3573520
0.6595679	310.000	46.123	34.910	21.524	3.202	2.424	2.3377692
0.6629699	315.000	46.867	35.473	22.087	3.286	2.487	2.3187945
0.6663143	320.000	47.611	36.036	22.655	3.371	2.551	2.3004009
0.6696026	325.000	48.354	36.599	23.227	3.456	2.616	2.2825637
0.6728364	330.000	49.098	37.162	23.803	3.541	2.681	2.2652572
0.6760169	335.000	49.842	37.725	24.384	3.628	2.746	2.2484606
0.6791455	340.000	50.586	38.288	24.969	3.715	2.812	2.2321518
0.6822236	345.000	51.330	38.851	25.558	3.803	2.878	2.2163109
0.6852523	350.000	52.074	39.415	26.151	3.891	2.945	2.2009187
0.6882328	355.000	52.818	39.978	26.749	3.980	3.012	2.1859573
0.6911663	360.000	53.562	40.541	27.351	4.069	3.080	2.1714096

Table A-1 K. E., Residual Range, and Total Ionization
of p, π and μ (continued)

β (v/c)	T (MeV)			R(cm)			i [$\frac{\text{MeV-cm}^2}{\text{gm}}$]
	p	π	μ	p	π	μ	
0.6940539	365.000	54.306	41.104	27.956	4.159	3.148	2.1572593
0.6968968	370.000	55.050	41.667	28.566	4.250	3.217	2.1434913
0.6996958	375.000	55.794	42.230	29.179	4.341	3.286	2.1300906
0.7024522	380.000	56.537	42.793	29.796	4.433	3.355	2.1170438
0.7051667	385.000	57.281	43.356	30.417	4.526	3.425	2.1043376
0.7078404	390.000	58.025	43.919	31.042	4.618	3.496	2.0919596
0.7104742	395.000	58.769	44.482	31.670	4.712	3.566	2.0798977
0.7130689	400.000	59.513	45.045	32.302	4.806	3.638	2.0681407
0.7156255	405.000	60.257	45.608	32.937	4.901	3.709	2.0566777
0.7181447	410.000	61.001	46.171	33.576	4.996	3.781	2.0454986
0.7206274	415.000	61.745	46.734	34.219	5.091	3.853	2.0345934
0.7230744	420.000	62.489	47.297	34.865	5.187	3.926	2.0237528
0.7254864	425.000	63.233	47.861	35.514	5.284	4.000	2.0135678
0.7278640	430.000	63.977	48.424	36.166	5.381	4.073	2.0034299
0.7302082	435.000	64.721	48.987	36.822	5.479	4.147	1.9935308
0.7325195	440.000	65.464	49.550	37.481	5.577	4.221	1.9838629
0.7347987	445.000	66.208	50.113	38.144	5.675	4.295	1.9744185
0.7370463	450.000	66.952	50.676	38.809	5.774	4.370	1.9651907
0.7392630	455.000	67.696	51.239	39.477	5.874	4.446	1.9561723
0.7414495	460.000	68.440	51.802	40.149	5.973	4.521	1.9473570
0.7436063	465.000	69.184	52.365	40.823	6.074	4.597	1.9387383
0.7457341	470.000	69.928	52.928	41.501	6.175	4.674	1.9303103
0.7478334	475.000	70.672	53.491	42.181	6.276	4.750	1.9220671
0.7499047	480.000	71.416	54.054	42.865	6.378	4.827	1.9140032
0.7519486	485.000	72.160	54.617	43.551	6.480	4.904	1.9061131
0.7539656	490.000	72.904	55.180	44.240	6.582	4.982	1.8983913
0.7559562	495.000	73.648	55.743	44.931	6.685	5.060	1.8908343
0.7579210	500.000	74.391	56.307	45.626	6.788	5.138	1.8834360
0.7598604	505.000	75.135	56.870	46.323	6.892	5.217	1.8761920
0.7617749	510.000	75.879	57.433	47.023	6.996	5.295	1.8690982
0.7636649	515.000	76.623	57.996	47.726	7.101	5.375	1.8621502
0.7655309	520.000	77.367	58.559	48.431	7.206	5.454	1.8553441
0.7673733	525.000	78.111	59.122	49.138	7.311	5.534	1.8486757
0.7691926	530.000	78.855	59.685	49.847	7.417	5.614	1.8421414
0.7709892	535.000	79.599	60.248	50.561	7.523	5.694	1.8357375
0.7727635	540.000	80.343	60.811	51.276	7.629	5.774	1.8294606
0.7745159	545.000	81.087	61.374	51.994	7.736	5.855	1.8233070
0.7762467	550.000	81.831	61.937	52.714	7.843	5.936	1.8172737
0.7779564	555.000	82.574	62.500	53.436	7.950	6.018	1.8113575
0.7796453	560.000	83.318	63.063	54.161	8.058	6.099	1.8055552
0.7813138	565.000	84.062	63.626	54.888	8.166	6.181	1.7998640
0.7829622	570.000	84.806	64.189	55.617	8.275	6.263	1.7942810
0.7845909	575.000	85.550	64.752	56.349	8.384	6.346	1.7888034
0.7862002	580.000	86.294	65.316	57.083	8.493	6.428	1.7834286
0.7877904	585.000	87.038	65.879	57.819	8.602	6.511	1.7781540
0.7893619	590.000	87.782	66.442	58.557	8.712	6.594	1.7729771
0.7909150	595.000	88.526	67.005	59.297	8.822	6.678	1.7678954
0.7924499	600.000	89.270	67.568	60.040	8.933	6.761	1.7629068
0.7939670	605.000	90.014	68.131	60.784	9.044	6.845	1.7580089
0.7954666	610.000	90.758	68.694	61.531	9.155	6.929	1.7531994
0.7969490	615.000	91.501	69.257	62.279	9.266	7.013	1.7484764
0.7984144	620.000	92.245	69.820	63.030	9.378	7.098	1.7438378
0.7998631	625.000	92.989	70.383	63.782	9.490	7.183	1.7392814
0.8012954	630.000	93.733	70.946	64.537	9.602	7.268	1.7348056
0.8027116	635.000	94.477	71.509	65.293	9.715	7.353	1.7304083

Table A-1 K. E., Residual Range, and Total Ionization
of p, π and μ (continued)

β (v/c)	T (MeV)			R(cm)			i [$\frac{\text{MeV-cm}^2}{\text{gm}}$]
	p	π	μ	p	π	μ	
0.8041118	640.000	95.221	72.072	66.052	9.827	7.438	1.7260877
0.8054964	645.000	95.965	72.635	66.812	9.940	7.524	1.7218422
0.8068656	650.000	96.709	73.198	67.574	10.054	7.610	1.7176699
0.8082197	655.000	97.453	73.762	68.338	10.167	7.696	1.7135693
0.8095588	660.000	98.197	74.325	69.104	10.281	7.782	1.7095387
0.8108832	665.000	98.941	74.888	69.871	10.396	7.868	1.7055765
0.8121932	670.000	99.685	75.451	70.640	10.510	7.955	1.7016813
0.8134890	675.000	100.428	76.014	71.411	10.625	8.042	1.6978516
0.8147767	680.000	101.172	76.577	72.184	10.740	8.129	1.6940860
0.8160386	685.000	101.916	77.140	72.959	10.855	8.216	1.6903830
0.8172928	690.000	102.660	77.703	73.735	10.970	8.304	1.6867414
0.8185337	695.000	103.404	78.266	74.513	11.086	8.391	1.6831598
0.8197614	700.000	104.148	78.829	75.292	11.202	8.479	1.6796368
0.8209761	705.000	104.892	79.392	76.073	11.318	8.567	1.6761714
0.8221780	710.000	105.636	79.955	76.856	11.435	8.655	1.6727622
0.8233673	715.000	106.380	80.518	77.640	11.552	8.743	1.6694082
0.8245441	720.000	107.124	81.081	78.426	11.668	8.832	1.6661081
0.8257087	725.000	107.868	81.644	79.214	11.786	8.920	1.6628609
0.8268612	730.000	108.611	82.208	80.002	11.903	9.009	1.6596656
0.8280018	735.000	109.355	82.771	80.793	12.021	9.098	1.6565208
0.8291307	740.000	110.099	83.334	81.585	12.138	9.188	1.6534258
0.8302480	745.000	110.843	83.897	82.378	12.256	9.277	1.6503795
0.8313540	750.000	111.587	84.460	83.173	12.375	9.366	1.6473810
0.8324487	755.000	112.331	85.023	83.969	12.493	9.456	1.6444291
0.8335323	760.000	113.075	85.586	84.767	12.612	9.546	1.6415232
0.8346050	765.000	113.819	86.149	85.566	12.731	9.636	1.6386622
0.8356669	770.000	114.563	86.712	86.367	12.850	9.726	1.6358453
0.8367182	775.000	115.307	87.275	87.169	12.969	9.816	1.6330717
0.8377591	780.000	116.051	87.838	87.972	13.089	9.907	1.6303404
0.8387896	785.000	116.795	88.401	88.776	13.208	9.997	1.6276507
0.8398100	790.000	117.538	88.964	89.582	13.328	10.088	1.6250019
0.8408203	795.000	118.282	89.527	90.389	13.448	10.179	1.6223930
0.8418207	800.000	119.026	90.090	91.198	13.569	10.270	1.6198233
0.8428114	805.000	119.770	90.653	92.008	13.689	10.361	1.6172923
0.8437924	810.000	120.514	91.217	92.819	13.810	10.453	1.6147989
0.8447639	815.000	121.258	91.780	93.631	13.931	10.544	1.6123428
0.8457260	820.000	122.002	92.343	94.444	14.052	10.636	1.6099230
0.8466789	825.000	122.746	92.906	95.257	14.173	10.727	1.6075391
0.8476226	830.000	123.490	93.469	96.075	14.294	10.819	1.6051901
0.8485574	835.000	124.234	94.032	96.892	14.416	10.911	1.6028757
0.8494832	840.000	124.978	94.595	97.710	14.538	11.003	1.6005952
0.8504003	845.000	125.722	95.158	98.530	14.660	11.096	1.5983478
0.8513087	850.000	126.465	95.721	99.350	14.782	11.188	1.5961331
0.8522086	855.000	127.209	96.284	100.172	14.904	11.281	1.5939505
0.8531000	860.000	127.953	96.847	100.995	15.026	11.373	1.5917993
0.8539831	865.000	128.697	97.410	101.819	15.149	11.466	1.5896791
0.8548580	870.000	129.441	97.973	102.644	15.272	11.559	1.5875893
0.8557248	875.000	130.185	98.536	103.470	15.395	11.652	1.5855294
0.8565836	880.000	130.929	99.099	104.297	15.518	11.745	1.5834988
0.8574345	885.000	131.673	99.663	105.125	15.641	11.838	1.5814971
0.8582775	890.000	132.417	100.226	105.954	15.764	11.932	1.5795237
0.8591129	895.000	133.161	100.789	106.784	15.888	12.025	1.5775782
0.8599406	900.000	133.905	101.352	107.616	16.011	12.119	1.5756601
0.8607609	905.000	134.648	101.915	108.448	16.135	12.213	1.5737690
0.8615737	910.000	135.392	102.478	109.281	16.259	12.306	1.5719042

Table A-1 K. E., Residual Range, and Total Ionization
of p, π and μ (continued)

β (v/c)	T (MeV)			R(cm)			i [MeV-cm ²] gm
	p	π	μ	p	π	μ	
0.8623792	915.000	136.136	103.041	110.116	16.383	12.400	1.5700656
0.8631774	920.000	136.880	103.604	110.951	16.508	12.495	1.5682525
0.8639686	925.000	137.624	104.167	111.787	16.632	12.589	1.5664646
0.8647526	930.000	138.368	104.730	112.624	16.757	12.683	1.5647015
0.8655297	935.000	139.112	105.293	113.462	16.881	12.777	1.5629628
0.8662999	940.000	139.856	105.856	114.301	17.006	12.872	1.5612480
0.8670633	945.000	140.600	106.419	115.141	17.131	12.966	1.5595568
0.8678199	950.000	141.344	106.982	115.982	17.256	13.061	1.5578887
0.8685700	955.000	142.088	107.545	116.824	17.381	13.156	1.5562434
0.8693135	960.000	142.832	108.108	117.666	17.507	13.251	1.5546206
0.8700504	965.000	143.575	108.672	118.510	17.632	13.346	1.5530199
0.8707810	970.000	144.319	109.235	119.354	17.758	13.441	1.5514410
0.8715053	975.000	145.063	109.798	120.199	17.884	13.536	1.5498834
0.8722233	980.000	145.807	110.361	121.045	18.009	13.631	1.5483469
0.8729352	985.000	146.551	110.924	121.892	18.135	13.727	1.5468310
0.8736409	990.000	147.295	111.487	122.740	18.262	13.822	1.5453356
0.8743406	995.000	148.039	112.050	123.588	18.388	13.918	1.5438602
0.8750343	1000.000	148.783	112.613	124.438	18.514	14.013	1.5424047
0.8757222	1005.000	149.527	113.176	125.288	18.641	14.109	1.5409686
0.8764042	1010.000	150.271	113.739	126.139	18.767	14.205	1.5395517
0.8770805	1015.000	151.015	114.302	126.990	18.894	14.301	1.5381535
0.8777511	1020.000	151.758	114.865	127.843	19.021	14.397	1.5367740
0.8784160	1025.000	152.502	115.428	128.696	19.148	14.493	1.5354128
0.8790754	1030.000	153.246	115.991	129.550	19.275	14.589	1.5340696
0.8797293	1035.000	153.990	116.554	130.405	19.402	14.685	1.5327442
0.8803778	1040.000	154.734	117.118	131.260	19.529	14.782	1.5314362
0.8810209	1045.000	155.478	117.681	132.116	19.657	14.878	1.5301455
0.8816587	1050.000	156.222	118.244	132.973	19.784	14.975	1.5288717
0.8822913	1055.000	156.966	118.807	133.831	19.912	15.071	1.5276147
0.8829186	1060.000	157.710	119.370	134.689	20.039	15.168	1.5263741
0.8835408	1065.000	158.454	119.933	135.548	20.167	15.264	1.5251497
0.8841580	1070.000	159.198	120.496	136.408	20.295	15.361	1.5239414
0.8847701	1075.000	159.942	121.059	137.268	20.423	15.458	1.5227488
0.8853773	1080.000	160.685	121.622	138.129	20.551	15.555	1.5215717
0.8859796	1085.000	161.429	122.185	138.991	20.679	15.652	1.5204099
0.8865770	1090.000	162.173	122.748	139.853	20.808	15.749	1.5192632
0.8871696	1095.000	162.917	123.311	140.716	20.936	15.846	1.5181313
0.8877574	1100.000	163.661	123.874	141.580	21.065	15.944	1.5170141
0.8883406	1105.000	164.405	124.437	142.444	21.193	16.041	1.5159113
0.8889191	1110.000	165.149	125.000	143.309	21.322	16.138	1.5148228
0.8894930	1115.000	165.893	125.564	144.175	21.451	16.236	1.5137483
0.8900624	1120.000	166.637	126.127	145.041	21.580	16.333	1.5126877
0.8906273	1125.000	167.381	126.690	145.907	21.709	16.431	1.5116406
0.8911878	1130.000	168.125	127.253	146.775	21.838	16.529	1.5106071
0.8917438	1135.000	168.869	127.816	147.643	21.967	16.626	1.5095868
0.8922955	1140.000	169.612	128.379	148.511	22.096	16.724	1.5085796
0.8928429	1145.000	170.356	128.942	149.380	22.225	16.822	1.5075852
0.8933860	1150.000	171.100	129.505	150.250	22.355	16.920	1.5066036
0.8939249	1155.000	171.844	130.068	151.120	22.484	17.018	1.5056345
0.8944597	1160.000	172.588	130.631	151.991	22.614	17.116	1.5046778
0.8949903	1165.000	173.332	131.194	152.862	22.743	17.214	1.5037333
0.8955168	1170.000	174.076	131.757	153.734	22.873	17.312	1.5028009
0.8960393	1175.000	174.820	132.320	154.606	23.003	17.411	1.5018803
0.8965578	1180.000	175.564	132.883	155.479	23.133	17.509	1.5009714
0.8970724	1185.000	176.308	133.446	156.353	23.263	17.607	1.5000741

Table A-1 K. E., Residual Range, and Total Ionization
of p, π and μ (continued)

β (v/c)	T (MeV)			R(cm)			i [MeV-cm ²] gm
	p	π	μ	p	π	μ	
0.8975830	1190.000	177.052	134.009	157.227	23.393	17.706	1.4991882
0.8980898	1195.000	177.795	134.573	158.101	23.523	17.804	1.4983135
0.8985927	1200.000	178.539	135.136	158.976	23.653	17.903	1.4974499
0.8990918	1205.000	179.283	135.699	159.851	23.783	18.001	1.4965973
0.8995872	1210.000	180.027	136.262	160.727	23.913	18.100	1.4957554
0.9000789	1215.000	180.771	136.825	161.604	24.044	18.199	1.4949243
0.9005669	1220.000	181.515	137.388	162.481	24.174	18.277	1.4941037
0.9010512	1225.000	182.259	137.951	163.359	24.305	18.376	1.4932934
0.9015319	1230.000	183.003	138.514	164.236	24.436	18.475	1.4924934
0.9020091	1235.000	183.747	139.077	165.115	24.566	18.574	1.4917035
0.9024827	1240.000	184.491	139.640	165.993	24.697	18.673	1.4909236
0.9029529	1245.000	185.235	140.203	166.873	24.828	18.772	1.4901535
0.9034195	1250.000	185.979	140.766	167.752	24.959	18.871	1.4893932
0.9038828	1255.000	186.722	141.329	168.633	25.090	18.970	1.4886425
0.9043427	1260.000	187.466	141.892	169.513	25.221	19.069	1.4879012
0.9047992	1265.000	188.210	142.455	170.394	25.352	19.169	1.4871693
0.9052523	1270.000	188.954	143.017	171.276	25.483	19.268	1.4864466
0.9057022	1275.000	189.698	143.582	172.158	25.614	19.367	1.4857331
0.9061488	1280.000	190.442	144.145	173.040	25.745	19.467	1.4850285
0.9065922	1285.000	191.186	144.708	173.923	25.877	19.566	1.4843329
0.9070324	1290.000	191.930	145.271	174.806	26.008	19.665	1.4836461
0.9074695	1295.000	192.674	145.834	175.690	26.140	19.765	1.4829678
0.9079034	1300.000	193.418	146.397	176.574	26.271	19.864	1.4822982
0.9083342	1305.000	194.162	146.960	177.458	26.403	19.964	1.4816370
0.9087619	1310.000	194.906	147.523	178.343	26.534	20.064	1.4809841
0.9091866	1315.000	195.649	148.086	179.228	26.666	20.163	1.4803395
0.9096082	1320.000	196.393	148.649	180.113	26.798	20.263	1.4797031
0.9100269	1325.000	197.137	149.212	180.999	26.930	20.363	1.4790746
0.9104426	1330.000	197.881	149.775	181.886	27.061	20.463	1.4784541
0.9108554	1335.000	198.625	150.338	182.772	27.193	20.563	1.4778415
0.9112653	1340.000	199.369	150.901	183.659	27.325	20.662	1.4772366
0.9116724	1345.000	200.113	151.465	184.547	27.457	20.762	1.4766394
0.9120765	1350.000	200.857	152.028	185.434	27.589	20.862	1.4760497
0.9124779	1355.000	201.601	152.591	186.322	27.722	20.962	1.4754675
0.9128765	1360.000	202.345	153.154	187.211	27.854	21.062	1.4748927
0.9132723	1365.000	203.089	153.717	188.100	27.986	21.162	1.4743252
0.9136653	1370.000	203.832	154.280	188.989	28.118	21.263	1.4737649
0.9140557	1375.000	204.576	154.843	189.878	28.251	21.363	1.4732116
0.9144434	1380.000	205.320	155.406	190.768	28.383	21.463	1.4726655
0.9148284	1385.000	206.064	155.969	191.658	28.515	21.563	1.4721262
0.9152107	1390.000	206.808	156.532	192.549	28.648	21.663	1.4715939
0.9155905	1395.000	207.552	157.095	193.439	28.780	21.764	1.4710683
0.9159676	1400.000	208.296	157.658	194.331	28.913	21.864	1.4705494
0.9163422	1405.000	209.040	158.221	195.222	29.046	21.965	1.4700371
0.9167143	1410.000	209.784	158.784	196.114	29.178	22.065	1.4695314
0.9170838	1415.000	210.528	159.347	197.006	29.311	22.165	1.4690322
0.9174508	1420.000	211.272	159.910	197.898	29.444	22.266	1.4685394
0.9178154	1425.000	212.016	160.474	198.791	29.577	22.366	1.4680528
0.9181775	1430.000	212.759	161.037	199.683	29.709	22.467	1.4675725
0.9185372	1435.000	213.503	161.600	200.577	29.842	22.568	1.4670984
0.9188945	1440.000	214.247	162.163	201.470	29.975	22.668	1.4666304
0.9192494	1445.000	214.991	162.726	202.364	30.108	22.769	1.4661684
0.9196019	1450.000	215.735	163.289	203.258	30.241	22.869	1.4657124
0.9199521	1455.000	216.479	163.852	204.152	30.374	22.970	1.4652622
0.9203000	1460.000	217.223	164.415	205.047	30.507	23.071	1.4648180

Table A-1 K. E., Residual Range, and Total Ionization
of p, π and μ (continued)

β (v/c)	T (MeV)			R(cm)			i [$\frac{\text{MeV-cm}^2}{\text{gm}}$]
	p	π	μ	p	π	μ	
0.9206456	1465.000	217.967	164.978	205.942	30.641	23.192	1.4643794
0.9209889	1470.000	218.711	165.541	206.857	30.774	23.293	1.4639465
0.9213299	1475.000	219.455	166.104	207.732	30.907	23.393	1.4635193
0.9216687	1480.000	220.199	166.667	208.628	31.040	23.494	1.4630977
0.9220053	1485.000	220.943	167.230	209.524	31.174	23.595	1.4626815
0.9223397	1490.000	221.686	167.793	210.420	31.307	23.696	1.4622708
0.9226719	1495.000	222.430	168.356	211.316	31.440	23.797	1.4618655
0.9230019	1500.000	223.174	168.920	212.213	31.574	23.898	1.4614654
0.9233298	1505.000	223.918	169.483	213.110	31.707	23.999	1.4610706
0.9236556	1510.000	224.662	170.046	214.007	31.841	24.100	1.4606811
0.9239793	1515.000	225.406	170.609	214.904	31.974	24.201	1.4602967
0.9243009	1520.000	226.150	171.172	215.802	32.108	24.302	1.4599173
0.9246204	1525.000	226.894	171.735	216.700	32.241	24.403	1.4595430
0.9249379	1530.000	227.638	172.298	217.598	32.375	24.504	1.4591736
0.9252533	1535.000	228.382	172.861	218.496	32.509	24.606	1.4588092
0.9255667	1540.000	229.126	173.424	219.395	32.642	24.707	1.4584497
0.9258782	1545.000	229.869	173.987	220.294	32.776	24.808	1.4580949
0.9261876	1550.000	230.613	174.550	221.193	32.910	24.909	1.4577449
0.9264951	1555.000	231.357	175.113	222.092	33.043	25.010	1.4573996
0.9268006	1560.000	232.101	175.676	222.991	33.177	25.112	1.4570590
0.9271043	1565.000	232.845	176.239	223.891	33.311	25.213	1.4567229
0.9274060	1570.000	233.589	176.802	224.791	33.445	25.314	1.4563914
0.9277058	1575.000	234.333	177.366	225.691	33.579	25.416	1.4560644
0.9280037	1580.000	235.077	177.929	226.591	33.713	25.517	1.4557418
0.9282998	1585.000	235.821	178.492	227.491	33.847	25.618	1.4554237
0.9285940	1590.000	236.565	179.055	228.392	33.981	25.720	1.4551100
0.9288864	1595.000	237.309	179.618	229.293	34.115	25.821	1.4548005
0.9291769	1600.000	238.053	180.181	230.193	34.249	25.923	1.4544953
0.9294657	1605.000	238.796	180.744	231.095	34.383	26.024	1.4541943
0.9297527	1610.000	239.540	181.307	231.996	34.517	26.126	1.4538975
0.9300379	1615.000	240.284	181.870	232.898	34.651	26.227	1.4536048
0.9303213	1620.000	241.028	182.433	233.799	34.785	26.329	1.4533167
0.9306030	1625.000	241.772	182.996	234.701	34.920	26.430	1.4530317
0.9308830	1630.000	242.516	183.559	235.603	35.054	26.532	1.4527511
0.9311613	1635.000	243.260	184.122	236.506	35.188	26.634	1.4524745
0.9314378	1640.000	244.004	184.685	237.408	35.322	26.735	1.4522018
0.9317127	1645.000	244.748	185.248	238.311	35.457	26.837	1.4519330
0.9319859	1650.000	245.492	185.811	239.213	35.591	26.939	1.4516679
0.9322574	1655.000	246.236	186.375	240.116	35.725	27.040	1.4514068
0.9325273	1660.000	246.980	186.938	241.019	35.860	27.142	1.4511493
0.9327956	1665.000	247.723	187.501	241.922	35.994	27.244	1.4508956
0.9330623	1670.000	248.467	188.064	242.826	36.128	27.345	1.4506456
0.9333273	1675.000	249.211	188.627	243.729	36.263	27.447	1.4503991
0.9335908	1680.000	249.955	189.190	244.633	36.397	27.549	1.4501561
0.9338527	1685.000	250.699	189.753	245.537	36.532	27.651	1.4499171
0.9341130	1690.000	251.443	190.316	246.441	36.666	27.752	1.4496814
0.9343717	1695.000	252.187	190.879	247.345	36.801	27.854	1.4494491
0.9346289	1700.000	252.931	191.442	248.249	36.935	27.956	1.4492203
0.9348846	1705.000	253.675	192.005	249.154	37.070	28.058	1.4489949
0.9351388	1710.000	254.419	192.568	250.058	37.204	28.160	1.4487729
0.9353915	1715.000	255.163	193.131	250.963	37.339	28.262	1.4485543
0.9356426	1720.000	255.906	193.694	251.868	37.474	28.364	1.4483389
0.9358923	1725.000	256.650	194.257	252.773	37.608	28.466	1.4481269
0.9361406	1730.000	257.394	194.821	253.678	37.743	28.567	1.4479181
0.9363873	1735.000	258.138	195.384	254.583	37.878	28.669	1.4477125

Table A-1 K. E., Residual Range, and Total Ionization
of p, π and μ (continued)

β (v/c)	T (MeV)			R(cm)			i [$\frac{\text{MeV-cm}^2}{\text{gm}}$]
	p	π	μ	p	π	μ	
0.9366327	1740.000	258.882	195.947	255.489	38.012	28.771	1.44475101
0.9368765	1745.000	259.626	196.510	256.394	38.147	28.873	1.44473108
0.9371190	1750.000	260.370	197.073	257.300	38.282	28.975	1.44471146
0.9373601	1755.000	261.114	197.636	258.205	38.417	29.077	1.44469215
0.9375997	1760.000	261.858	198.199	259.111	38.551	29.179	1.44467315
0.9378380	1765.000	262.602	198.762	260.017	38.686	29.281	1.44465445
0.9380749	1770.000	263.346	199.325	260.923	38.821	29.383	1.44463605
0.9383104	1775.000	264.090	199.888	261.830	38.956	29.485	1.44461795
0.9385446	1780.000	264.833	200.451	262.736	39.091	29.587	1.44460014
0.9387774	1785.000	265.577	201.014	263.642	39.225	29.690	1.44458262
0.9390089	1790.000	266.321	201.577	264.549	39.360	29.792	1.44456538
0.9392390	1795.000	267.065	202.140	265.455	39.495	29.894	1.44454843
0.9394679	1800.000	267.809	202.703	266.362	39.630	29.996	1.44453176
0.9396954	1805.000	268.553	203.267	267.269	39.765	30.098	1.44451537
0.9399216	1810.000	269.297	203.830	268.176	39.900	30.200	1.44449926
0.9401466	1815.000	270.041	204.393	269.083	40.035	30.302	1.44448342
0.9403703	1820.000	270.785	204.956	269.990	40.170	30.404	1.44446785
0.9405927	1825.000	271.529	205.519	270.898	40.305	30.507	1.44445255
0.9408138	1830.000	272.273	206.082	271.805	40.440	30.609	1.44443752
0.9410338	1835.000	273.017	206.645	272.712	40.575	30.711	1.44442274
0.9412524	1840.000	273.760	207.208	273.620	40.710	30.813	1.44440823
0.9414699	1845.000	274.504	207.771	274.527	40.845	30.915	1.44439398
0.9416861	1850.000	275.248	208.334	275.435	40.980	31.018	1.44437996
0.9419011	1855.000	275.992	208.897	276.343	41.115	31.120	1.44436623
0.9421149	1860.000	276.736	209.460	277.251	41.250	31.222	1.44435274
0.9423276	1865.000	277.480	210.023	278.159	41.385	31.324	1.44433949
0.9425390	1870.000	278.224	210.586	279.067	41.520	31.427	1.44432648
0.9427493	1875.000	278.968	211.149	279.975	41.655	31.529	1.44431372
0.9429584	1880.000	279.712	211.712	280.883	41.791	31.631	1.44430120
0.9431663	1885.000	280.456	212.276	281.791	41.926	31.733	1.44428892
0.9433731	1890.000	281.200	212.839	282.700	42.061	31.836	1.44427688
0.9435788	1895.000	281.943	213.402	283.608	42.196	31.938	1.44426506
0.9437833	1900.000	282.687	213.965	284.517	42.331	32.040	1.44425348
0.9439867	1905.000	283.431	214.528	285.425	42.466	32.143	1.44424213
0.9441890	1910.000	284.175	215.091	286.334	42.602	32.245	1.44423101
0.9443902	1915.000	284.919	215.654	287.243	42.737	32.347	1.44422010
0.9445903	1920.000	285.663	216.217	288.152	42.872	32.450	1.44420943
0.9447893	1925.000	286.407	216.780	289.060	43.007	32.552	1.44419897
0.9449872	1930.000	287.151	217.343	289.969	43.142	32.654	1.44418874
0.9451841	1935.000	287.895	217.906	290.878	43.278	32.757	1.44417872
0.9453799	1940.000	288.639	218.469	291.787	43.413	32.859	1.44416891
0.9455746	1945.000	289.383	219.032	292.696	43.548	32.961	1.44415931
0.9457683	1950.000	290.127	219.595	293.606	43.683	33.064	1.44414992
0.9459609	1955.000	290.870	220.158	294.515	43.819	33.166	1.44414075
0.9461525	1960.000	291.614	220.722	295.424	43.954	33.269	1.44413178
0.9463431	1965.000	292.358	221.285	296.333	44.089	33.371	1.44412302
0.9465326	1970.000	293.102	221.848	297.243	44.225	33.473	1.44411445
0.9467212	1975.000	293.846	222.411	298.152	44.360	33.576	1.44410609
0.9469087	1980.000	294.590	222.974	299.062	44.495	33.678	1.44409792
0.9470952	1985.000	295.334	223.537	299.971	44.631	33.781	1.44408996
0.9472808	1990.000	296.078	224.100	300.881	44.766	33.883	1.44408219
0.9474653	1995.000	296.822	224.663	301.791	44.901	33.986	1.44407461
0.9476489	2000.000	297.566	225.226	302.700	45.037	34.088	1.44406722
0.9478315	2005.000	298.310	225.789	303.610	45.172	34.190	1.44406002
0.9480132	2010.000	299.054	226.352	304.520	45.307	34.293	1.44405301

Table A-1 K. E., Residual Range, and Total Ionization
of p, π and μ (continued)

β (v/c)	T (MeV)			R(cm)			i [$\frac{\text{MeV-cm}^2}{\text{gm}}$]
	p	π	μ	p	π	μ	
0.9481939	2015.000	299.797	226.915	305.430	45.443	34.395	1.4404618
0.9483736	2020.000	300.541	227.478	306.340	45.578	34.448	1.4403954
0.9485524	2025.000	301.285	228.041	307.250	45.713	34.600	1.4403309
0.9487303	2030.000	302.029	228.604	308.159	45.849	34.703	1.4402681
0.9489072	2035.000	302.773	229.167	309.069	45.984	34.805	1.4402071
0.9490832	2040.000	303.517	229.731	309.980	46.120	34.908	1.4401479
0.9492583	2045.000	304.261	230.294	310.890	46.255	35.010	1.4400905
0.9494325	2050.000	305.005	230.857	311.800	46.390	35.113	1.4400346
0.9496058	2055.000	305.749	231.420	312.710	46.526	35.215	1.4399808
0.9497781	2060.000	306.493	231.983	313.620	46.661	35.318	1.4399285
0.9499496	2065.000	307.237	232.546	314.530	46.797	35.420	1.4398779
0.9501202	2070.000	307.980	233.109	315.440	46.932	35.523	1.4398291
0.9502900	2075.000	308.724	233.672	316.351	47.068	35.625	1.4397819
0.9504588	2080.000	309.468	234.235	317.261	47.203	35.728	1.4397362
0.9506268	2085.000	310.212	234.798	318.171	47.338	35.830	1.4396923
0.9507939	2090.000	310.956	235.361	319.082	47.474	35.933	1.4396500
0.9509602	2095.000	311.700	235.924	319.992	47.609	36.035	1.4396093
0.9511256	2100.000	312.444	236.487	320.903	47.745	36.138	1.4395701
0.9512902	2105.000	313.188	237.050	321.813	47.880	36.240	1.4395325
0.9514539	2110.000	313.932	237.613	322.723	48.016	36.343	1.4394966
0.9516168	2115.000	314.676	238.177	323.634	48.151	36.445	1.4394621
0.9517789	2120.000	315.420	238.740	324.544	48.287	36.548	1.4394292
0.9519402	2125.000	316.164	239.303	325.455	48.422	36.650	1.4393978
0.9521006	2130.000	316.907	239.866	326.365	48.558	36.753	1.4393679
0.9522603	2135.000	317.651	240.429	327.276	48.693	36.856	1.4393395
0.9524191	2140.000	318.395	240.992	328.187	48.829	36.958	1.4393125
0.9525771	2145.000	319.139	241.555	329.097	48.964	37.061	1.4392871
0.9527344	2150.000	319.883	242.118	330.008	49.099	37.163	1.4392631
0.9528908	2155.000	320.627	242.681	330.918	49.235	37.266	1.4392405
0.9530465	2160.000	321.371	243.244	331.829	49.370	37.368	1.4392193
0.9532014	2165.000	322.115	243.807	332.740	49.506	37.471	1.4391996
0.9533555	2170.000	322.859	244.370	333.650	49.641	37.573	1.4391813
0.9535089	2175.000	323.603	244.933	334.561	49.777	37.676	1.4391643
0.9536615	2180.000	324.347	245.496	335.472	49.912	37.778	1.4391487
0.9538133	2185.000	325.091	246.059	336.382	50.048	37.881	1.4391345
0.9539644	2190.000	325.834	246.623	337.293	50.183	37.984	1.4391216
0.9541148	2195.000	326.578	247.186	338.204	50.319	38.086	1.4391100
0.9542644	2200.000	327.322	247.749	339.114	50.454	38.189	1.4390999
0.9544132	2205.000	328.066	248.312	340.025	50.590	38.291	1.4390909
0.9545614	2210.000	328.810	248.875	340.936	50.725	38.394	1.4390833
0.9547087	2215.000	329.554	249.438	341.847	50.861	38.496	1.4390771
0.9548554	2220.000	330.298	250.001	342.757	50.996	38.599	1.4390720
0.9550014	2225.000	331.042	250.564	343.668	51.132	38.702	1.4390683
0.9551467	2230.000	331.786	251.127	344.579	51.267	38.804	1.4390657
0.9552912	2235.000	332.530	251.690	345.490	51.403	38.907	1.4390645
0.9554350	2240.000	333.274	252.253	346.400	51.538	39.009	1.4390645
0.9555782	2245.000	334.017	252.816	347.311	51.674	39.112	1.4390657
0.9557206	2250.000	334.761	253.379	348.222	51.809	39.214	1.4390681
0.9558624	2255.000	335.505	253.942	349.133	51.945	39.317	1.4390717
0.9560035	2260.000	336.249	254.505	350.043	52.080	39.419	1.4390765
0.9561438	2265.000	336.993	255.068	350.954	52.216	39.522	1.4390825
0.9562836	2270.000	337.737	255.632	351.865	52.351	39.625	1.4390896
0.9564226	2275.000	338.481	256.195	352.775	52.487	39.727	1.4390980
0.9565610	2280.000	339.225	256.758	353.686	52.622	39.830	1.4391074
0.9566987	2285.000	339.969	257.321	354.597	52.758	39.932	1.4391181

Table A-1 K. E., Residual Range, and Total Ionization
of p, π and μ (continued)

β (v/c)	T (MeV)			R(cm)			i [$\frac{\text{MeV-cm}^2}{\text{gm}}$]
	p	π	μ	p	π	μ	
0.9568357	2290.000	340.713	257.884	355.508	52.893	40.035	1.4371298
0.9569722	2295.000	341.457	258.447	356.418	53.029	40.137	1.4391426
0.9571079	2300.000	342.201	259.010	357.329	53.164	40.240	1.4391566
0.9572430	2305.000	342.944	259.573	358.240	53.300	40.342	1.4391716
0.9573774	2310.000	343.688	260.136	359.150	53.435	40.445	1.4391878
0.9575113	2315.000	344.432	260.699	360.061	53.571	40.548	1.4392051
0.9576445	2320.000	345.176	261.262	360.972	53.706	40.650	1.4392233
0.9577770	2325.000	345.920	261.825	361.882	53.842	40.753	1.4392427
0.9579090	2330.000	346.664	262.388	362.793	53.977	40.855	1.4392631
0.9580403	2335.000	347.408	262.951	363.703	54.113	40.958	1.4392846
0.9581710	2340.000	348.152	263.514	364.614	54.248	41.060	1.4393071
0.9583010	2345.000	348.896	264.078	365.525	54.384	41.163	1.4393306
0.9584305	2350.000	349.640	264.641	366.435	54.519	41.265	1.4393551
0.9585593	2355.000	350.384	265.204	367.346	54.655	41.368	1.4393807
0.9586876	2360.000	351.128	265.767	368.256	54.790	41.470	1.4394072
0.9588153	2365.000	351.871	266.330	369.167	54.926	41.573	1.4394347
0.9589423	2370.000	352.615	266.893	370.077	55.061	41.676	1.4394632
0.9590688	2375.000	353.359	267.456	370.988	55.197	41.778	1.4394928
0.9591947	2380.000	354.103	268.019	371.899	55.332	41.881	1.4395232
0.9593200	2385.000	354.847	268.582	372.809	55.468	41.983	1.4395546
0.9594447	2390.000	355.591	269.145	373.719	55.603	42.086	1.4395870
0.9595688	2395.000	356.335	269.708	374.630	55.738	42.188	1.4396202
0.9596924	2400.000	357.079	270.271	375.540	55.874	42.291	1.4396545
0.9598154	2405.000	357.823	270.834	376.450	56.009	42.393	1.4396896
0.9599378	2410.000	358.567	271.397	377.361	56.145	42.496	1.4397257
0.9600597	2415.000	359.311	271.960	378.271	56.280	42.598	1.4397627
0.9601810	2420.000	360.054	272.524	379.181	56.416	42.701	1.4398005
0.9603018	2425.000	360.798	273.087	380.091	56.551	42.803	1.4398392
0.9604220	2430.000	361.542	273.650	381.002	56.687	42.906	1.4398789
0.9605416	2435.000	362.286	274.213	381.912	56.822	43.008	1.4399194
0.9606607	2440.000	363.030	274.776	382.822	56.957	43.111	1.4399608
0.9607793	2445.000	363.774	275.339	383.732	57.093	43.213	1.4400031
0.9608973	2450.000	364.518	275.902	384.642	57.228	43.316	1.4400462
0.9610148	2455.000	365.262	276.465	385.552	57.364	43.418	1.4400901
0.9611318	2460.000	366.006	277.028	386.463	57.499	43.521	1.4401349
0.9612482	2465.000	366.750	277.591	387.373	57.634	43.623	1.4401806
0.9613641	2470.000	367.494	278.154	388.283	57.770	43.726	1.4402270
0.9614795	2475.000	368.238	278.717	389.193	57.905	43.828	1.4402743
0.9615943	2480.000	368.981	279.280	390.103	58.041	43.931	1.4403223
0.9617087	2485.000	369.725	279.843	391.012	58.176	44.033	1.4403712
0.9618225	2490.000	370.469	280.406	391.922	58.311	44.136	1.4404209
0.9619358	2495.000	371.213	280.969	392.832	58.447	44.238	1.4404714
0.9620486	2500.000	371.957	281.532	393.742	58.582	44.340	1.4405226
0.9621609	2505.000	372.701	282.095	394.652	58.717	44.443	1.4405746
0.9622727	2510.000	373.445	282.658	395.562	58.853	44.545	1.4406274
0.9623840	2515.000	374.189	283.222	396.471	58.988	44.648	1.4406810
0.9624949	2520.000	374.933	283.785	397.381	59.123	44.750	1.4407353
0.9626052	2525.000	375.677	284.348	398.291	59.259	44.853	1.4407904
0.9627150	2530.000	376.421	284.911	399.200	59.394	44.955	1.4408462
0.9628243	2535.000	377.165	285.474	400.110	59.530	45.058	1.4409027
0.9629332	2540.000	377.908	286.037	401.020	59.665	45.160	1.4409600
0.9630416	2545.000	378.652	286.600	401.929	59.800	45.262	1.4410180
0.9631495	2550.000	379.396	287.163	402.839	59.935	45.365	1.4410767
0.9632569	2555.000	380.140	287.726	403.748	60.071	45.467	1.4411362
0.9633639	2560.000	380.884	288.289	404.657	60.206	45.570	1.4411963

Table A-1 K. E., Residual Range, and Total Ionization
of p, π and μ (continued)

β (v/c)	T (MeV)			R(cm)			i [$\frac{\text{MeV-cm}^2}{\text{gm}}$]
	p	π	μ	p	π	μ	
0.9634703	2565.000	381.628	288.852	405.567	60.341	45.672	1.4412571
0.9635764	2570.000	382.372	287.415	406.476	60.477	45.775	1.4413187
0.9636819	2575.000	383.116	289.977	407.385	60.612	45.877	1.4413807
0.9637870	2580.000	383.860	290.542	408.295	60.747	45.979	1.4414438
0.9638916	2585.000	384.604	291.105	409.204	60.883	46.082	1.4415074
0.9639958	2590.000	385.348	291.668	410.113	61.018	46.184	1.4415717
0.9640996	2595.000	386.091	292.231	411.022	61.153	46.286	1.4416365
0.9642028	2600.000	386.835	292.794	411.931	61.288	46.389	1.4417022
0.9643057	2605.000	387.579	293.357	412.840	61.424	46.491	1.4417684
0.9644080	2610.000	388.323	293.920	413.749	61.559	46.594	1.4418353
0.9645100	2615.000	389.067	294.483	414.658	61.694	46.696	1.4419028
0.9646115	2620.000	389.811	295.046	415.567	61.829	46.798	1.4419710
0.9647125	2625.000	390.555	295.609	416.476	61.965	46.901	1.4420397
0.9648132	2630.000	391.299	296.172	417.385	62.100	47.003	1.4421092
0.9649134	2635.000	392.043	296.735	418.294	62.235	47.105	1.4421792
0.9650131	2640.000	392.787	297.298	419.203	62.370	47.208	1.4422498
0.9651125	2645.000	393.531	297.861	420.111	62.505	47.310	1.4423211
0.9652114	2650.000	394.275	298.425	421.020	62.641	47.412	1.4423930
0.9653099	2655.000	395.018	298.988	421.929	62.776	47.515	1.4424655
0.9654079	2660.000	395.762	299.551	422.837	62.911	47.617	1.4425386
0.9655056	2665.000	396.506	300.114	423.746	63.046	47.719	1.4426123
0.9656028	2670.000	397.250	300.677	424.654	63.181	47.822	1.4426865
0.9656996	2675.000	397.994	301.240	425.563	63.316	47.924	1.4427613
0.9657961	2680.000	398.738	301.803	426.471	63.452	48.026	1.4428367
0.9658920	2685.000	399.482	302.366	427.379	63.587	48.128	1.4429127
0.9659877	2690.000	400.226	302.929	428.288	63.722	48.231	1.4429892
0.9660828	2695.000	400.970	303.492	429.196	63.857	48.333	1.4430663
0.9661776	2700.000	401.714	304.055	430.104	63.992	48.435	1.4431440
0.9662720	2705.000	402.458	304.618	431.012	64.127	48.538	1.4432222
0.9663660	2710.000	403.202	305.181	431.920	64.262	48.640	1.4433009
0.9664596	2715.000	403.946	305.744	432.828	64.397	48.742	1.4433802
0.9665528	2720.000	404.689	306.307	433.736	64.533	48.844	1.4434601
0.9666456	2725.000	405.433	306.870	434.644	64.668	48.947	1.4435404
0.9667381	2730.000	406.177	307.434	435.552	64.803	49.049	1.4436213
0.9668301	2735.000	406.921	307.997	436.460	64.938	49.151	1.4437027
0.9669218	2740.000	407.665	308.560	437.368	65.073	49.253	1.4437847
0.9670131	2745.000	408.409	309.123	438.275	65.208	49.356	1.4438671
0.9671040	2750.000	409.153	309.686	439.183	65.343	49.458	1.4439501
0.9671945	2755.000	409.897	310.249	440.091	65.478	49.560	1.4440335
0.9672846	2760.000	410.641	310.812	440.998	65.613	49.662	1.4441175
0.9673744	2765.000	411.385	311.375	441.906	65.748	49.764	1.4442020
0.9674638	2770.000	412.128	311.938	442.813	65.883	49.867	1.4442869
0.9675528	2775.000	412.872	312.501	443.721	66.018	49.969	1.4443724
0.9676415	2780.000	413.616	313.064	444.628	66.153	50.071	1.4444583
0.9677298	2785.000	414.360	313.627	445.535	66.288	50.173	1.4445447
0.9678177	2790.000	415.104	314.190	446.443	66.423	50.275	1.4446316
0.9679053	2795.000	415.848	314.751	447.350	66.558	50.377	1.4447190
0.9679925	2800.000	416.592	315.316	448.257	66.693	50.480	1.4448068
0.9680794	2805.000	417.336	315.880	449.164	66.828	50.582	1.4448951
0.9681659	2810.000	418.080	316.443	450.071	66.963	50.684	1.4449839
0.9682520	2815.000	418.824	317.006	450.978	67.098	50.786	1.4450731
0.9683378	2820.000	419.568	317.569	451.885	67.233	50.888	1.4451628
0.9684233	2825.000	420.312	318.132	452.792	67.368	50.990	1.4452529
0.9685084	2830.000	421.055	318.695	453.699	67.503	51.092	1.4453434
0.9685932	2835.000	421.799	319.258	454.605	67.637	51.194	1.4454344

Table A-1 K. E., Residual Range, and Total Ionization
of p, π and μ (continued)

β (v/c)	T (MeV)			R (cm)			i [$\frac{\text{MeV-cm}^2}{\text{gm}}$]
	p	π	μ	p	π	μ	
0.9686776	2840.000	422.543	319.821	455.512	67.772	51.297	1.4455259
0.9687616	2845.000	423.287	320.384	456.419	67.967	51.399	1.4456178
0.9688454	2850.000	424.031	320.947	457.325	68.042	51.501	1.4457100
0.9689288	2855.000	424.775	321.510	458.232	68.177	51.603	1.4458028
0.9690118	2860.000	425.519	322.073	459.138	68.312	51.705	1.4458959
0.9690945	2865.000	426.263	322.636	460.045	68.447	51.807	1.4459895
0.9691769	2870.000	427.007	323.199	460.951	68.582	51.909	1.4460835
0.9692590	2875.000	427.751	323.762	461.857	68.716	52.011	1.4461779
0.9693407	2880.000	428.495	324.325	462.764	68.851	52.113	1.4462727
0.9694221	2885.000	429.239	324.887	463.670	68.986	52.215	1.4463679
0.9695032	2890.000	429.982	325.452	464.576	69.121	52.317	1.4464635
0.9695840	2895.000	430.726	326.015	465.482	69.256	52.419	1.4465595
0.9696644	2900.000	431.470	326.578	466.388	69.391	52.521	1.4466559
0.9697445	2905.000	432.214	327.141	467.294	69.525	52.623	1.4467527
0.9698243	2910.000	432.958	327.704	468.200	69.660	52.725	1.4468499
0.9699038	2915.000	433.702	328.267	469.106	69.795	52.827	1.4469475
0.9699829	2920.000	434.446	328.830	470.011	69.930	52.929	1.4470454
0.9700618	2925.000	435.190	329.393	470.917	70.064	53.031	1.4471438
0.9701403	2930.000	435.934	329.956	471.823	70.199	53.133	1.4472425
0.9702185	2935.000	436.678	330.519	472.728	70.334	53.235	1.4473415
0.9702965	2940.000	437.422	331.082	473.634	70.469	53.337	1.4474410
0.9703741	2945.000	438.165	331.645	474.539	70.603	53.439	1.4475408
0.9704514	2950.000	438.909	332.208	475.445	70.738	53.541	1.4476410
0.9705284	2955.000	439.653	332.771	476.350	70.873	53.643	1.4477415
0.9706051	2960.000	440.397	333.335	477.255	71.007	53.745	1.4478424
0.9706815	2965.000	441.141	333.898	478.160	71.142	53.847	1.4479436
0.9707576	2970.000	441.885	334.461	479.065	71.277	53.949	1.4480452
0.9708334	2975.000	442.629	335.024	479.970	71.411	54.051	1.4481472
0.9709089	2980.000	443.373	335.587	480.875	71.546	54.153	1.4482494
0.9709841	2985.000	444.117	336.150	481.780	71.681	54.255	1.4483520
0.9710590	2990.000	444.861	336.713	482.685	71.815	54.357	1.4484550
0.9711336	2995.000	445.605	337.276	483.590	71.950	54.459	1.4485583
0.9712080	3000.000	446.349	337.839	484.495	72.085	54.560	1.4486619
0.9712820	3005.000	447.092	338.402	485.399	72.219	54.662	1.4487658
0.9713558	3010.000	447.836	338.965	486.304	72.354	54.764	1.4488701
0.9714293	3015.000	448.580	339.528	487.209	72.488	54.866	1.4489747
0.9715025	3020.000	449.324	340.091	488.113	72.623	54.968	1.4490796
0.9715754	3025.000	450.068	340.654	489.018	72.757	55.070	1.4491848
0.9716480	3030.000	450.812	341.217	489.922	72.892	55.172	1.4492904
0.9717204	3035.000	451.556	341.781	490.826	73.027	55.273	1.4493963
0.9717924	3040.000	452.300	342.344	491.730	73.161	55.375	1.4495024
0.9718642	3045.000	453.044	342.907	492.634	73.296	55.477	1.4496089
0.9719357	3050.000	453.788	343.470	493.539	73.430	55.579	1.4497157
0.9720070	3055.000	454.532	344.033	494.443	73.565	55.681	1.4498228
0.9720780	3060.000	455.276	344.596	495.347	73.699	55.782	1.4499302
0.9721487	3065.000	456.019	345.159	496.250	73.834	55.884	1.4500378
0.9722191	3070.000	456.763	345.722	497.154	73.968	55.986	1.4501459
0.9722893	3075.000	457.507	346.285	498.058	74.102	56.088	1.4502541
0.9723592	3080.000	458.251	346.848	498.962	74.237	56.190	1.4503627
0.9724288	3085.000	458.995	347.411	499.865	74.371	56.291	1.4504715
0.9724982	3090.000	459.739	347.974	500.769	74.506	56.393	1.4505806
0.9725673	3095.000	460.483	348.537	501.672	74.640	56.495	1.4506900
0.9726361	3100.000	461.227	349.100	502.576	74.775	56.597	1.4507997
0.9727047	3105.000	461.971	349.663	503.479	74.909	56.698	1.4509096
0.9727730	3110.000	462.715	350.226	504.382	75.043	56.800	1.4510199

Table A-1 K. E., Residual Range, and Total Ionization
of p, π and μ (continued)

β (v/c)	T (MeV)			R(cm)			i [MeV-cm ²] gm
	p	π	μ	p	π	μ	
0.9728411	3115.000	463.459	350.790	505.286	75.178	56.902	1.4511304
0.9729089	3120.000	464.202	351.353	506.189	75.317	57.003	1.4512411
0.9729765	3125.000	464.946	351.916	507.092	75.447	57.105	1.4513521
0.9730438	3130.000	465.690	352.479	507.995	75.581	57.207	1.4514634
0.9731108	3135.000	466.434	353.042	508.898	75.715	57.308	1.4515750
0.9731776	3140.000	467.178	353.605	509.800	75.850	57.410	1.4516868
0.9732442	3145.000	467.922	354.168	510.703	75.984	57.512	1.4517989
0.9733105	3150.000	468.666	354.731	511.606	76.118	57.613	1.4519112
0.9733765	3155.000	469.410	355.294	512.507	76.252	57.715	1.4520238
0.9734424	3160.000	470.154	355.857	513.411	76.387	57.817	1.4521366
0.9735079	3165.000	470.898	356.420	514.314	76.521	57.918	1.4522497
0.9735732	3170.000	471.642	356.983	515.216	76.655	58.020	1.4523630
0.9736383	3175.000	472.386	357.546	516.119	76.790	58.122	1.4524766
0.9737032	3180.000	473.129	358.109	517.021	76.924	58.223	1.4525904
0.9737678	3185.000	473.873	358.672	517.923	77.058	58.325	1.4527044
0.9738321	3190.000	474.617	359.236	518.825	77.192	58.426	1.4528187
0.9738962	3195.000	475.361	359.799	519.727	77.326	58.528	1.4529332
0.9739601	3200.000	476.105	360.362	520.629	77.461	58.630	1.4530480
0.9740238	3205.000	476.849	360.925	521.531	77.595	58.731	1.4531630
0.9740872	3210.000	477.593	361.488	522.433	77.729	58.833	1.4532782
0.9741504	3215.000	478.337	362.051	523.335	77.863	58.934	1.4533936
0.9742133	3220.000	479.081	362.614	524.237	77.997	59.036	1.4535092
0.9742760	3225.000	479.825	363.177	525.138	78.132	59.137	1.4536251
0.9743385	3230.000	480.569	363.740	526.040	78.266	59.239	1.4537412
0.9744008	3235.000	481.312	364.303	526.941	78.400	59.340	1.4538575
0.9744628	3240.000	482.056	364.866	527.843	78.534	59.442	1.4539741
0.9745246	3245.000	482.800	365.429	528.744	78.668	59.543	1.4540908
0.9745862	3250.000	483.544	365.992	529.645	78.802	59.645	1.4542078
0.9746476	3255.000	484.288	366.555	530.547	78.936	59.746	1.4543249
0.9747087	3260.000	485.032	367.118	531.448	79.070	59.848	1.4544423
0.9747696	3265.000	485.776	367.682	532.349	79.204	59.949	1.4545599
0.9748303	3270.000	486.520	368.245	533.250	79.338	60.051	1.4546777
0.9748908	3275.000	487.264	368.808	534.151	79.472	60.152	1.4547956
0.9749510	3280.000	488.008	369.371	535.052	79.606	60.254	1.4549138
0.9750111	3285.000	488.752	369.934	535.952	79.741	60.355	1.4550323
0.9750709	3290.000	489.496	370.497	536.853	79.875	60.457	1.4551508
0.9751305	3295.000	490.239	371.060	537.754	80.009	60.558	1.4552696
0.9751899	3300.000	490.983	371.623	538.654	80.143	60.659	1.4553886
0.9752491	3305.000	491.727	372.186	539.555	80.276	60.761	1.4555077
0.9753080	3310.000	492.471	372.749	540.455	80.410	60.862	1.4556271
0.9753668	3315.000	493.215	373.312	541.356	80.544	60.964	1.4557467
0.9754253	3320.000	493.959	373.875	542.256	80.678	61.065	1.4558663
0.9754837	3325.000	494.703	374.438	543.156	80.812	61.166	1.4559862
0.9755418	3330.000	495.447	375.001	544.056	80.946	61.268	1.4561064
0.9755997	3335.000	496.191	375.564	544.956	81.080	61.369	1.4562266
0.9756574	3340.000	496.935	376.127	545.856	81.214	61.471	1.4563471
0.9757149	3345.000	497.679	376.691	546.756	81.348	61.572	1.4564677
0.9757722	3350.000	498.423	377.254	547.656	81.482	61.673	1.4565885
0.9758293	3355.000	499.166	377.817	548.556	81.616	61.774	1.4567094
0.9758862	3360.000	499.910	378.380	549.455	81.750	61.876	1.4568306
0.9759429	3365.000	500.654	378.943	550.355	81.883	61.977	1.4569520
0.9759994	3370.000	501.398	379.506	551.254	82.017	62.078	1.4570734
0.9760557	3375.000	502.142	380.069	552.154	82.151	62.180	1.4571951
0.9761118	3380.000	502.886	380.632	553.053	82.285	62.281	1.4573169
0.9761677	3385.000	503.630	381.195	553.952	82.419	62.382	1.4574389

Table A-1 K. E., Residual Range, and Total Ionization
of p, π and μ (continued)

β (v/c)	T(MeV)			R(cm)			i [MeV-cm ²] gm
	p	π	μ	p	π	μ	
0.9762234	3390.000	504.374	381.758	554.852	82.552	62.484	1.4575611
0.9762789	3395.000	505.118	382.321	555.751	82.686	62.585	1.4576833
0.9763342	3400.000	505.862	382.884	556.650	82.820	62.686	1.4578057
0.9763893	3405.000	506.606	383.447	557.549	82.954	62.787	1.4579284
0.9764443	3410.000	507.349	384.010	558.448	63.087	62.888	1.4580512
0.9764990	3415.000	508.093	384.573	559.347	83.221	62.990	1.4581741
0.9765535	3420.000	508.837	385.137	560.245	83.355	63.091	1.4582973
0.9766079	3425.000	509.581	385.700	561.144	83.489	63.192	1.4584205
0.9766620	3430.000	510.325	386.263	562.043	83.622	63.293	1.4585438
0.9767160	3435.000	511.069	386.826	562.941	83.756	63.395	1.4586674
0.9767698	3440.000	511.813	387.389	563.840	83.890	63.496	1.4587911
0.9768234	3445.000	512.557	387.952	564.738	84.023	63.597	1.4589149
0.9768768	3450.000	513.301	388.515	565.636	84.157	63.698	1.4590389
0.9769300	3455.000	514.045	389.078	566.535	84.291	63.799	1.4591630
0.9769831	3460.000	514.789	389.641	567.433	84.424	63.900	1.4592872
0.9770359	3465.000	515.533	390.204	568.331	84.558	64.001	1.4594116
0.9770886	3470.000	516.276	390.767	569.229	84.691	64.103	1.4595362
0.9771411	3475.000	517.020	391.330	570.127	84.825	64.204	1.4596608
0.9771934	3480.000	517.764	391.893	571.025	84.959	64.305	1.4597851
0.9772455	3485.000	518.508	392.456	571.922	85.092	64.406	1.4599106
0.9772975	3490.000	519.252	393.019	572.820	85.226	64.507	1.4600357
0.9773493	3495.000	519.996	393.583	573.718	85.359	64.608	1.4601609
0.9774009	3500.000	520.740	394.146	574.615	85.493	64.709	1.4602862
0.9774523	3505.000	521.484	394.709	575.513	85.626	64.810	1.4604117
0.9775035	3510.000	522.228	395.272	576.410	85.760	64.911	1.4605372
0.9775546	3515.000	522.972	395.835	577.307	85.893	65.012	1.4606630
0.9776055	3520.000	523.716	396.398	578.205	86.027	65.113	1.4607888
0.9776562	3525.000	524.460	396.961	579.102	86.160	65.214	1.4609148
0.9777068	3530.000	525.203	397.524	579.999	86.294	65.315	1.4610409
0.9777571	3535.000	525.947	398.087	580.896	86.427	65.416	1.4611671
0.9778073	3540.000	526.691	398.650	581.793	86.561	65.517	1.4612934
0.9778574	3545.000	527.435	399.213	582.690	86.694	65.618	1.4614199
0.9779072	3550.000	528.179	399.776	583.586	86.828	65.719	1.4615465
0.9779569	3555.000	528.923	400.339	584.483	86.961	65.820	1.4616731
0.9780065	3560.000	529.667	400.902	585.380	87.094	65.921	1.4617999
0.9780558	3565.000	530.411	401.465	586.276	87.228	66.022	1.4619268
0.9781050	3570.000	531.155	402.028	587.173	87.361	66.123	1.4620538
0.9781540	3575.000	531.899	402.592	588.069	87.495	66.224	1.4621810
0.9782029	3580.000	532.643	403.155	588.965	87.628	66.325	1.4623082
0.9782516	3585.000	533.386	403.718	589.862	87.761	66.426	1.4624355

Appendix II Energy Spectra of $K_{\mu 3}$ and τ'

The energy spectra of $K_{\mu 3}$ and τ' have been studied by other research groups²¹⁻²³. More than one form has been proposed for each spectrum under different hypotheses of interaction matrix elements. The energy spectra which we have chosen and normalized to unity for the analyses carried out in Chapters II and III are those having the best experimental support^{22,23}. The normalized spectra are reproduced in Figs. A-4^{21,22} and A-5²³ as a handy reference.

In order to check the effect of uncertainties in these spectra on our results, several varied energy spectra for τ' and $K_{\mu 3}$ have been generated respectively by varying the related parameter within its error range²³ and by using our measured ratio $K_{\mu 3}/K_{e 3}$. The effect has been found negligible.

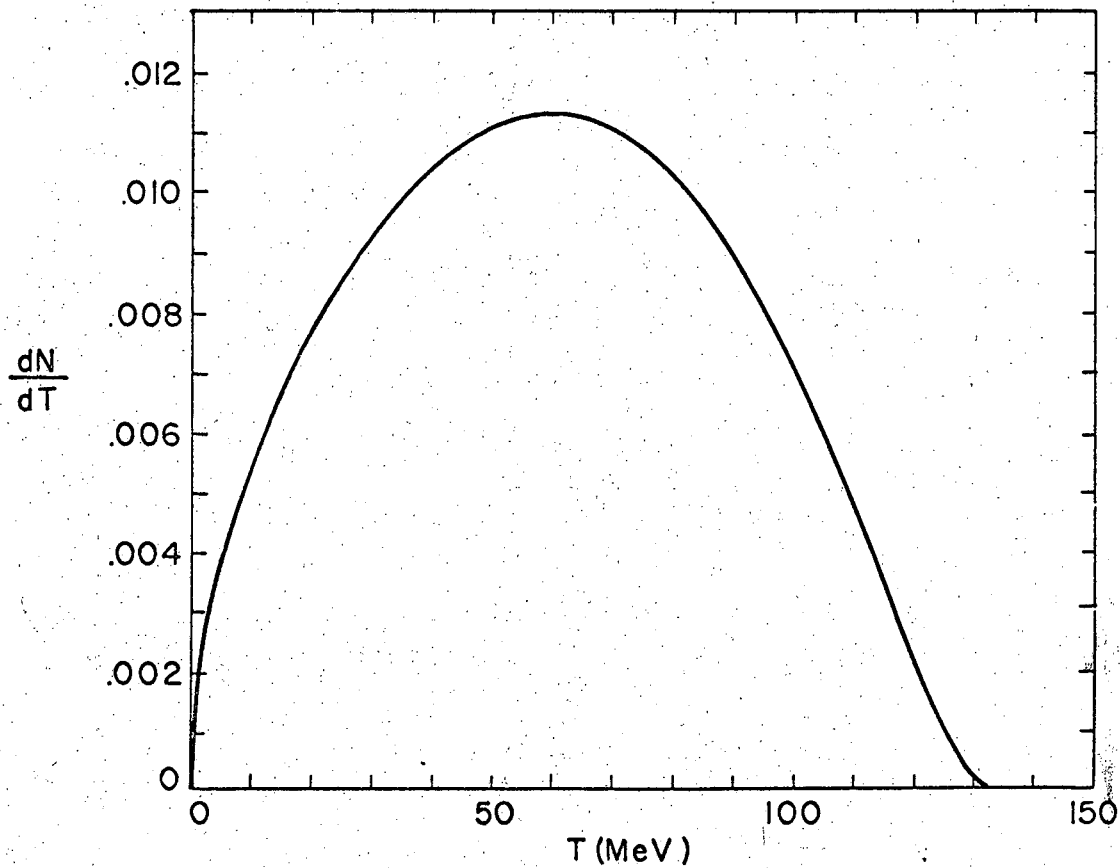


Fig. A-4 Energy Spectrum of $K_{\mu 3}$ as Function
of K.E. of μ^+

MU-36594

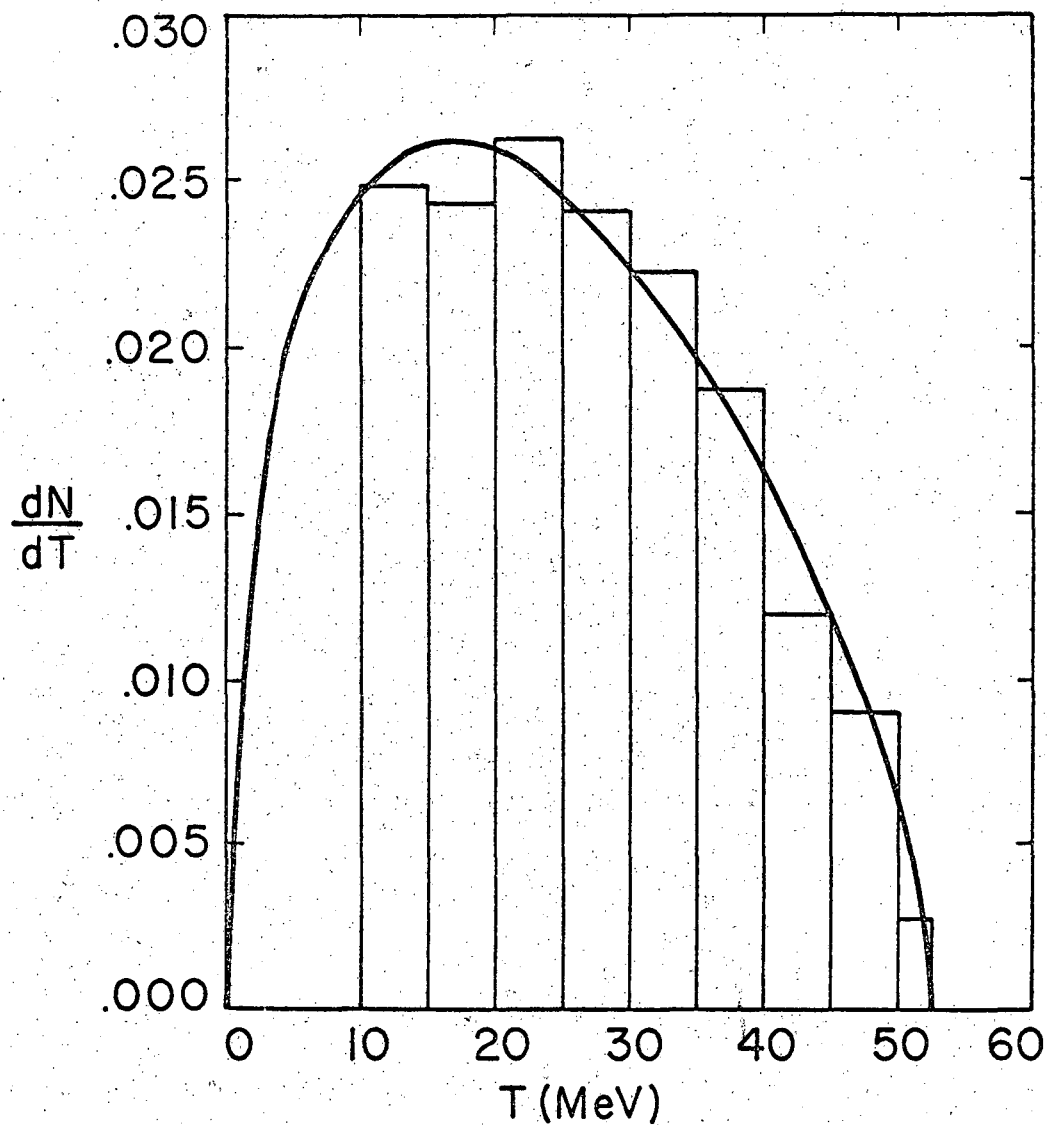


Fig. A-5 Energy Spectrum of τ'
as Function of K.E. of π^+

MU-36630

Appendix III Positrons in the Experiment

In this appendix we shall elaborate the evaluation of two important quantities related to the positrons in this experiment. One is the mean blob density of the e^+ tracks of K_{e3} events, and the other is the number of e^+ tracks produced around the scan volume in the stack.

(a) Mean Blob Density of the e^+ Tracks of K_{e3} Events: The relative efficiency for finding a K_{e3} was defined in Chapter III by Eq.

(3-12):

$$\bar{\epsilon}_{e3} = \int_{B_{\min}}^{B_{\max}} \left[1 - m(B_{25} - B) \right] \frac{dN}{dB} dB \quad (3-12)$$

which can be simplified by normalizing $\frac{dN}{dB}$ to unity into the following form

$$\bar{\epsilon}_{e3} = 1 - mB_{25} + \int_{B_{\min}}^{B_{\max}} B \frac{dN}{dB} dB$$

where m is to be determined.

To evaluate the integral contained in the above equation, we might first think of the technique indicated in Eq. (3-19). However, this technique is not applicable although the energy spectrum $\frac{dT}{dB}$ for the K_{e3} is known^{21,22}. The reason for this is that the positron range is poorly defined¹³ on an individual basis because of radiative loss of energy. In other words, the quantity $\frac{dT}{dB}$ cannot be easily defined as in the case of π or μ (i.e. by measuring both the range of a track and its blob density at its origin and by use of a range-energy curve such as shown in Fig. A-2). For this reason we have to resort to a purely empirical method.

By the definition of $\frac{dN}{dB} dB$ (See Chapter III), we can interpret

the integral as follows:

$$\int_{B_{\min}}^{B_{\max}} B \frac{dN}{dB} dB \equiv \bar{B} \text{ (Mean blob density for the } e^+ \text{ tracks of the } K_{e3} \text{ events)}$$

The value of \bar{B} can be determined by measuring the blob density at K^+ decay point of each e^+ track for all K_{e3} events and taking the average of the measurements. As the result of our blob counting for the K_{e3} events, we have obtained

$$\bar{B} \sim 17.81$$

or

$$\int_{B_{\min}}^{B_{\max}} B \frac{dN}{dB} dB \sim 17.81 \quad (A-3)$$

where an approximation is made because not all K_{e3} events contained in the sample have been observed.

By substituting Eq. (A-3) and the value of B_{25} (i.e. 38.64 blobs/100 μ) into Eq. (3-12), we obtain Eq. (3-20) which relates $\bar{\epsilon}_{e3}$ to m in a simple way.

(b) Average Ratio between e^\pm and $(\pi + \mu)$ Tracks around the Scan

Volume: As the final products of all decay modes of K^+ meson are e^\pm and ν , it is essential to know the spatial distribution of the e^\pm tracks in order to evaluate the number of possible errors in the first track following. Although the analysis carried out below is a rough approximation, it proves to be useful in the quick evaluation performed in Chapter III.

(i) Mean Energy, Mean Free Path for the γ and e^\pm in Different

Decay Modes: From the energy spectra of different decay modes, we

are able to list the mean energy^{21,24} of the π^0 and the related mean energy for γ and for the pair production in Table A-2.

Table A-2 Mean Energy, Mean Free Path¹⁴ and Approximate Range¹³ of γ and e^\pm

Decay Mode	E or \bar{E} (MeV) (Mean Energy)			$\bar{\lambda}_\gamma$ (cm) (Mean Free Path of γ)	\bar{R}_e (cm) (Approximate Range of e^\pm)
	π^0	γ	e^\pm		
$K_{\mu 3} \rightarrow \mu \pi^0 \nu$ \swarrow 2γ \searrow $4e$	220	110	55	5.04	4.6
$K_{e 3} \rightarrow e \pi^0 \nu$ \swarrow $4e$	240	120	60	5.01	4.9
$K_{\pi 2} \rightarrow \pi^+ \pi^0$ \swarrow $4e$ \searrow $\mu^+ \rightarrow e^+$	245	123	62	5.00	4.9
$\tau^+ \rightarrow \pi^+ \pi^0 \pi^0$ \swarrow $8e$ \searrow e^+	35 165	18 83	9 42	13.00 6.76	1.4 3.8

(ii) Number of e^\pm Tracks Produced per 100 K^+ Mesons at Different R: *8-17-67*

As the scan volume is small compared with the whole stack, it can be considered a point source of all secondaries. Then the total number of the e^\pm tracks produced from all the modes at a distance R' from the scan volume can be expressed by:



$$\begin{aligned}
 n_e(R') = 100 & \left[4r'_{\mu 3} (1 - e^{-R'/5.04}) + 4r'_{e 3} (1 - e^{-R'/5.01}) \right. \\
 & + 2r'_{\pi 2} (1 - e^{-R'/5.00}) + 8r'_{\tau'} (1 - e^{-R'/13.0}) \\
 & \left. + 2r'_{\tau} \quad \quad \quad + \quad \quad \quad r'_{\tau'} \quad \quad \quad \right] \quad (A-4) \\
 & \quad \quad \quad \text{(from } 2\pi^+) \quad \quad \quad \text{(from } 1\pi^+)
 \end{aligned}$$

Hence the increment of the e^\pm track between R' and $R' + dR'$ can be calculated by taking $(dn_e/dR')dR'$. Since all the e^\pm tracks cannot travel indefinitely without annihilation or absorption in emulsion, we have to make corrections for this effect. For simplicity, let us suppose all e^\pm tracks produced from all the modes had a single range of 4.5 cm. Then we obtain the total number of e^\pm tracks at different R as

$$N_e(R) = \int_0^R H[(R' + 4.5) - R] \frac{dn_e}{dR'} dR' \quad (A-5)$$

$$\text{where } H[(R' + 4.5) - R] = \begin{cases} 1 & \text{at } R < R' + 4.5 \text{ cm} \\ 0 & \text{at } R \geq R' + 4.5 \text{ cm} \end{cases} \quad (A-6)$$

After performing the numerical integration of (A-5) we obtain $N_e(R)$ as a function of R , which is plotted in Fig. A-6.

(iii) Number of π^+ and μ^+ Tracks at Different R' from All Modes:

By neglecting the small contribution due to τ and τ' , we can estimate $N_\pi(R)$ from $K_{\pi 2}$ by considering the fact that a π track with 23 blobs/100 μ or of a residual range ~ 4.3 cm (i.e. 1.5 minimum ionization) could not be mistaken for an e^\pm track of minimum ionization. In other words, we would include a π track from $K_{\pi 2}$ for only 7.7 cm. We thus obtain



$$N_{\pi}(R) = r'_{\pi 2} H[7.7 - R] = 19.3 H[7.7 - R] \quad (A-7)$$

$$\text{where } H[7.7 - R] = \begin{cases} 1 & \text{at } R < 7.7 \text{ cm,} \\ 0 & \text{at } R \geq 7.7 \text{ cm.} \end{cases} \quad (A-8)$$

For the spacial distribution of μ tracks, we consider that all μ tracks either from $K_{\mu 2}$ or $K_{\mu 3}$ could be mistaken within a distance of 12.5 cm for e^{\pm} . We may thus write down $N_{\mu}(R)$ as

$$N_{\mu}(R) = r'_{\mu 2} + r'_{\mu 3} = 61.8 + 5.4 = 67.2 \quad (A-9)$$

The distributions N_{π} and N_{μ} are plotted in Fig. A-6.

(iv) Average Ratio Between N_e and $(N_{\pi} + N_{\mu})$: From Fig. A-6 we can evaluate the average ratio between N_e and $(N_{\pi} + N_{\mu})$ over a distance from $R = 0$ to $R = 12.5$ cm. The results lead to

$$\frac{\int_0^{12.5 \text{ cm}} \frac{N_e(R)}{[N_{\pi}(R) + N_{\mu}(R)]} dR}{\int_0^{12.5 \text{ cm}} dR} = 36\% \quad (A-10)$$

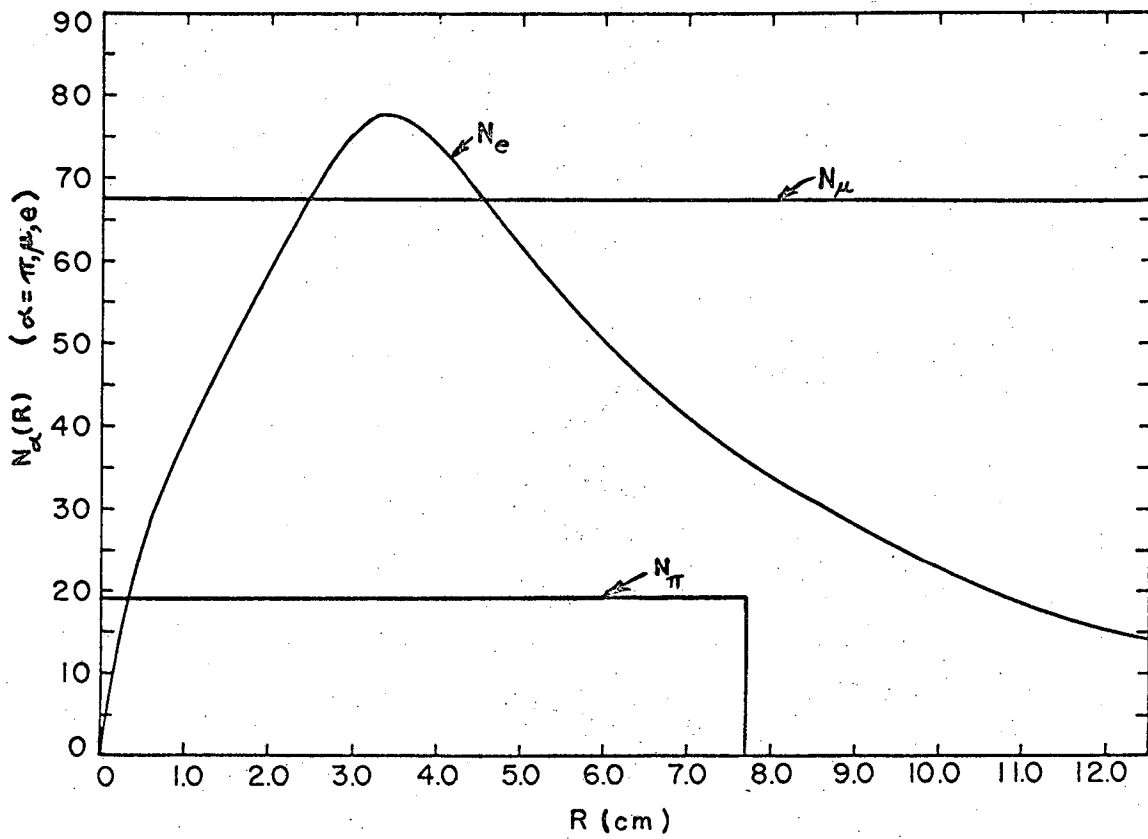


Fig. A-6 No. of π , μ and e^\pm Produced Around Scan Volume as Functions of Distance from the Volume.

Appendix IV π -Decays in Flight

The possible number of π -decays in flight among $K_{\pi 2}$ events in this experiment is evaluated here. The result shows that we may expect 2 or 3 π -decays in flight. Since none of these decays in flight have been observed among our 134 $K_{\pi 2}$ events, some of them may have been mistaken for $K_{\mu 3}$ and some included in the lost or out of stack events. Because of the negligible effect of this number on our branching ratios, no particular effort was needed to search for such events. The evaluation is described below as a reference.

Let $N_{d.f.} \equiv$ No. of π 's decaying in flight in a total of $N_{\pi 2}$ events. By definition, $N_{d.f.}$ can be related to $N_{\pi 2}$ by the following equation:

$$N_{d.f.} = N_{\pi 2} (1 - e^{-t/\tau}) \quad (A-11)$$

where $N_{\pi 2} \equiv$ No. of $K_{\pi 2}$ (includes both π decaying at rest and in flight)

$$t \approx \frac{m_{\pi}}{m_p} 2.84 \times 10^{-9} \text{ sec (Moderation time for a 108.6 MeV } \pi \text{ from } K_{\pi 2} \text{)}^{25}$$

and

$$\tau = 2.55 \times 10^{-8} \text{ sec (Life time of } \pi^+ \text{)}^{26}$$

By approximating $N_{\pi 2} \approx 134$, we obtain

$$N_{d.f.} \approx 134 (1 - e^{-0.0166}) = 2.28 \quad (A-12)$$



REFERENCES

1. Byron P. Roe, Daniel Sinclair, John L. Brown, Donald A. Glaser, John A. Kadyk, and George H. Trilling, New Determination of the K^+ decay Branching Ratios, Phys. Rev. Letters 7, 346 (1961).
2. Francis S. Shaklee, Gary L. Jensen, Byron P. Roe, and Daniel Sinclair, Branching Ratios of the K^+ Meson, Phys. Rev. 136, B1423 (1964).
3. R. W. Birge, D. H. Perkins, J. R. Peterson, D. H. Störk and M. N. Whitehead, Decay Characteristics and Masses of Positive K Mesons Produced by the Bevatron, Nuovo Cimento 4, 834 (1956).
4. G. Alexander, R. H. W. Johnson and C. O'Ceallaigh, Nuovo Cimento 6, 478 (1957).
5. T. E. Hoang, M. F. Kaplon, and G. Yekutieli, Ratios of Decay Modes of K^+ Mesons Produced by the Cosmotron, Phys. Rev. 102, 1185 (1956).
6. P. K. Aditya, J. K. Bøggild, K. H. Hansen, J. E. Hooper and M. Scharff, Observations on the Decay of K^+ Mesons, in Proceedings of the Cosmic Ray Symposium (Ahmedabad, India, 1960), NP-11232, p. 373.
7. Allen E. Everett, Evidence on the existence of Shadow Pions in K^+ Decay, Phys. Rev. Letters 14, 615 (1965).
8. C. F. Powell, P. H. Powell, and D. H. Perkins, The Study of Elementary Particles by the Photographic Method (Pergamon Press, New York, London, Paris and Los Angeles, 1959), Sec. 9.
9. H. H. Heckman, F. M. Smith and W. H. Barkas, The Masses of Positive K-Particles, Nuovo Cimento 3, 85 (1956).



10. L. W. Alvarez and S. Goldhaber, The Lifetime of the τ -Meson, *Nuovo Cimento* 2, 344 (1955).
11. V. Fitch and R. Motley, Mean Life of K^+ Mesons, *Phys. Rev.* 101, 496 (1956).
12. Luis W. Alvarez, Frank S. Crawford, Myron L. Good, and M. Lynn Stevenson, Lifetime of K Mesons, *Phys. Rev.* 101, 503 (1956).
13. Martin J. Berger and Stephen M. Seltzer, Tables of Energy-Losses and Ranges of Electrons and Positrons, in Studies in Penetration of Charged Particles in Matter (National Academy of Sciences -- National Research Council, Washington, D. C., 1964), Publication 1133, p. 205.
14. Walter H. Barkas, Nuclear Research Emulsions, Vol. II, Chap. 5 (to be published).
15. Masao Sugawara, (Physics Department, Purdue University, Lafayette, Indiana), private communication.
16. H. Chew, Evidence against Partially Conserved Currents in K_{13}^+ Decay, *Phys. Rev. Letters* 8, 297 (1962).
17. R. H. Dalitz, Isotopic Spin Changes in τ and θ Decay, *Proc. Phys. Soc. (London)* A69, 527 (1956).
18. Walter H. Barkas, Nuclear Research Emulsions (Academic Press, New York and London, 1963), Vol. I, Chap. 9.
19. W. H. Barkas, P. H. Barrett, P. Cüer, H. H. Heckman, F. M. Smith and H. K. Ticho, The Range-Energy Relation in Emulsion, *Nuovo Cimento* 8, 185 (1958).
20. Walter H. Barkas and Martin J. Berger, Tables of Energy Losses and Ranges of Heavy Charged Particles, in Studies in Penetration of Charged Particles in Matter (National Academy of Sciences --

National Research Council, Washington, D. C., 1964), Publication 1133, p. 103.

21. N. Brene, L. Egardt and B. Qvist, On the $K_{\mu 3}^-$ and $K_{e 3}^-$ Decay Modes, Nucl. Phys. 22, 553 (1961).
22. John L. Brown, John A. Kadyk, George H. Trilling, and Remy T. Van de Walle, Byron P. Roe, and Daniel Sinclair, Experimental studies of the Form Factors in $K_{\mu 3}^+$ and $K_{e 3}^+$ Decay, Phys. Rev. Letters 8, 450 (1962).
23. George E. Kalmus, Anne Kernan, Robert T. Pu, Wilson M. Powell, and Richard Dowd, Energy Spectrum of π^+ in $K^+ \rightarrow \pi^+ \pi^0 \pi^0$ Decay, Phys. Rev. Letters 13, 99 (1964).
24. John L. Brown, John A. Kadyk, George H. Trilling, Remy T. Van de Walle, Byron P. Roe and Daniel Sinclair, Experimental Study of the $K_{e 3}^+$ Decay Interaction, Phys. Rev. Letters 7, 423 (1961).
25. Walter H. Barkas and D. M. Young, Emulsion Tables, I., Heavy-Particle Functions, University of California Radiation Laboratory Report UCRL-2579 Rev., September 1954 (unpublished).
26. Arthur H. Rosenfeld, Angela Barbaro-Galtieri, Walter H. Barkas, Pierre L. Bastien, Janos Kirz, and Matts Roos, Data on Elementary Particles and Resonant States, Rev. of Mod. Phys. 36, 977 (1964).

This report was prepared as an account of Government sponsored work. Neither the United States, nor the Commission, nor any person acting on behalf of the Commission:

- A. Makes any warranty or representation, expressed or implied, with respect to the accuracy, completeness, or usefulness of the information contained in this report, or that the use of any information, apparatus, method, or process disclosed in this report may not infringe privately owned rights; or
- B. Assumes any liabilities with respect to the use of, or for damages resulting from the use of any information, apparatus, method, or process disclosed in this report.

As used in the above, "person acting on behalf of the Commission" includes any employee or contractor of the Commission, or employee of such contractor, to the extent that such employee or contractor of the Commission, or employee of such contractor prepares, disseminates, or provides access to, any information pursuant to his employment or contract with the Commission, or his employment with such contractor.

[Faint, illegible text covering the majority of the page]

